UNIVERSITÀ
DEGLI STUDI
DI PADOVA

Università degli Studi di Padova

Department of Neurosciences

Ph.D. Course in Translational Specialistic Medicine "G.B. Morgagni"

Curriculum: Neurosciences

XXXI Cycle

# Restoration of auditory network after Cochlear Implant: A P300 and EEG study using LORETA (Low resolution brain electromagnetic tomography)

**Coordinator:** Prof. Annalisa Angelini

**Supervisor**: Prof. Alessandro Martini

**Ph.D. student**: Dr. Flavia Gheller

Academic year 2017-2018

# Table of contents

# List of Tables



# List of Figures

## Abstract

The proper functioning of the auditory processing needs an integration of many types of information, and a synchronised action between auditory cortex and other cortical and subcortical centres. The normal development of connectivity between the auditory system and the higher neurocognitive functions depends on sensory experience, and congenital hearing loss makes it essentially impossible.

The aim of this work was to perform an electrophysiological analysis of auditory cortical areas in patients with cochlear implant (CI).

Thirty implanted patients were included in the study. Twenty-four of them were prelingual patients and they were divided into three groups, according to the age at time of CI surgery and to the duration of CI use: group A - early implant and lengthy CI use, group B - late implant and lengthy CI use, group C - late implant and short CI use. The remaining six patients were affected by postlingual deafness, and they were included in the group D. Each patient group was compared with a normal hearing age matched control group. Each subject underwent an Event-related potentials (ERPs) evaluation and electroencephalographic registration. All data analysis were performed by using Loreta software (Low Resolution Electromagnetic Tomography).

ERPs latencies were for the most part significantly longer in patients than in controls. Concerning the Event-related cortical activity, all the control groups showed a high and well-defined activation in frontals areas and the cingulate cortex, in the N200 and P300 time windows. A comparable activation in strength and timing, between patients and controls, was only found in the first prelingual patient group (A), and to a lesser extent in the second group (B), while patients belonging to the third prelingual group (C) showed a very low cortical activation, with no cyclic pattern. Postlingual patients (D) showed no difference in activation compared to controls.

ln a second step of the study, functional connectivity was analysed from EEG data, in two different conditions: resting state and activation state. Default mode network, left and right Precuneus and associative visual cortex were examined. No difference between prelingual patients and controls was found in the first group (A). Functional connectivity showed a significant increase in the second (B) and third (C) prelingual patient group, especially in the activation state, and specifically between visual areas and Precuneus and posterior cingulate cortex, while postlingual patients (D) showed no difference compared to controls.

Cochlear implant adds a new auditory modality in prelingual patients, allowing the creation of a functional network. This involves the areas implicated in sensory and cognitive modalities, and needs some time to form. The duration of CI use is crucial: prolonged CI use, in addiction to an early time of implant, can restore auditory network, allowing a normalization process, from both an audiological and a neurophysiological point of view. However, in the case of patients with postlingual hearing loss, cochlear implant seems to restore and reinforce a cortical network that has already been formed, before the onset of the hearing impairment.

# 1. Deafness and Restoration of the Auditory System

## 1.1 Anatomy notes

The auditory system is the sensory system responsible for the sense of hearing.
It includes the peripheral system, whose main structures are the outer, middle, and inner ear, and the central auditory system, that goes from the cochlear nucleus to the auditory cortex.
The hearing process begins with the vibrations reaching the outer ear and ends with their interpretation as sound in the temporal lobe.

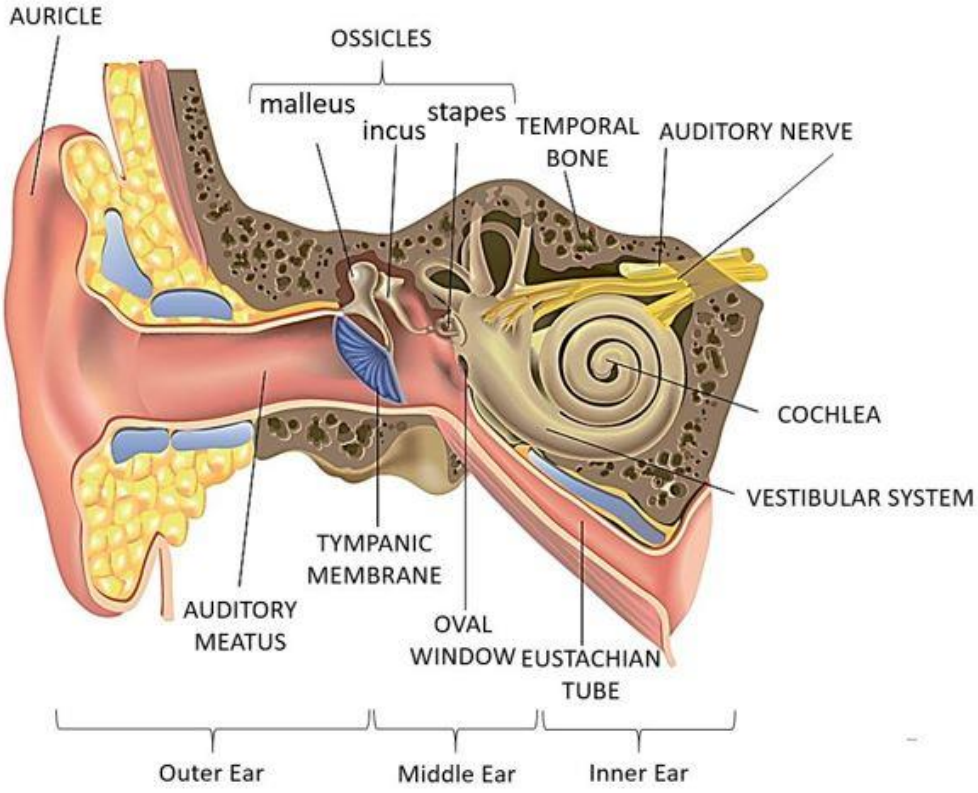


*Figure 2.1.1 Anatomy of the human ear*. Treccani - Enciclopedia della Scienza e della Tecnica (2007)

- Outer ear

This consists of the visible part called the auricle and the external auditory meatus, a canal from the auricle to the tympanic membrane.
The outer ear picks up sound waves from the external environment and then directs them from the air to the tympanic membrane.

The latter is a thin and flexible membrane that separates the external ear from the middle ear. Its function is to receive sound vibrations and transmit them to the ossicles inside the middle ear.

- Middle ear

This is the portion of the ear between the tympanic membrane and the oval window.
It transmits sound vibrations from the outer ear to the inner ear.
This part of the ear includes three tiny bones (so-called ossicles: malleus, incus, and stapes), the oval and round windows, and the Eustachian tube.
Acoustic pressure waves strike the tympanic membrane, making it vibrate, and these vibrations are transmitted by the ossicles into the inner ear, through the oval window.
The oval window covers the entrance to the cochlea in the inner ear, and the Eustachian tube has the role of equalizing the pressure on both sides of the tympanic membrane.

- Inner ear

The inner part has a key role in detecting sound and maintaining balance.
It consists of a cavity in the temporal bone, the bony labyrinth, which is separated into three different sections: the vestibule (responsible for balance), the semi-circular canals, and the cochlea. (Emanuel et al, 2009)

Cochlea

Once the sound vibrations of the tympanic membrane have been transmitted to the oval window through the three ossicles, the sound waves are transmitted to the cochlea, where they are transformed into electrical impulses which are sent to the brain. In this final phase of the auditory process, the electrical signal is translated into recognisable and understandable sounds. (Alberti, 2001)

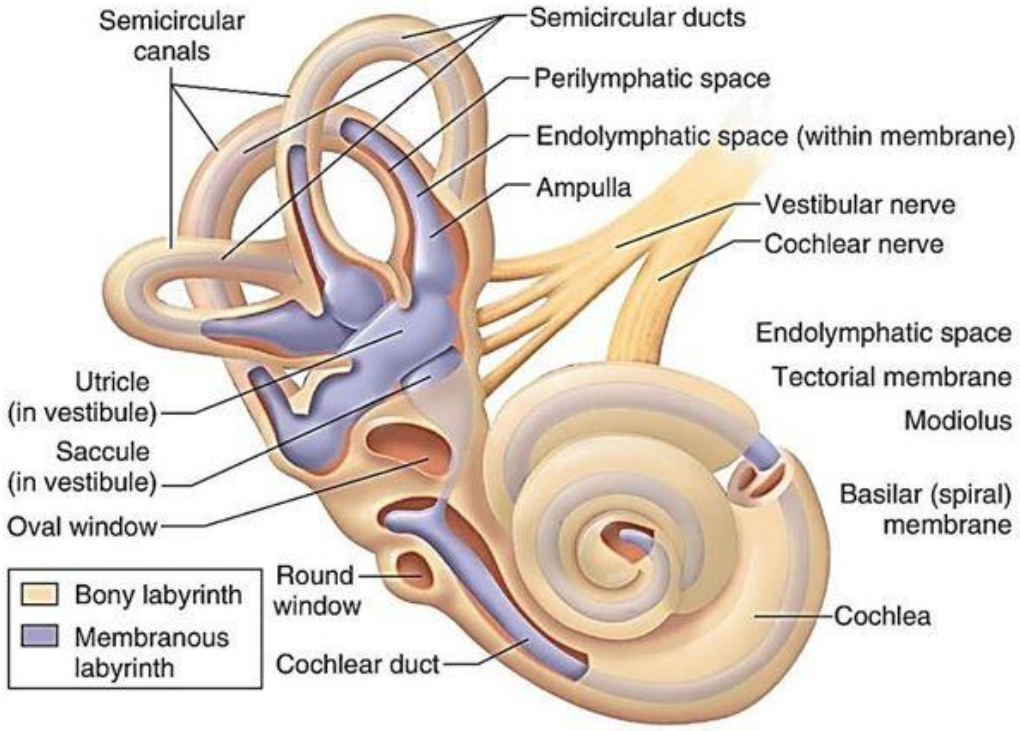


*Figure 1.1.2. Anatomy of the human cochlea.* Kevin T. Patton K, Thibodeau G. A. Science Health Science Division. 2010; Elsevier

The cochlea has the function of converting sound vibrations into electrical signals. It is composed of three canals coiled around a bony axis, the modiolus: the vestibular duct, the tympanic duct, and the cochlear duct (scala vestibuli, scala tympani and scala media). All three are filled with fluid.

The tympanic duct and the vestibular duct are filled with perilymph and they are linked through the part of the cochlear labyrinth called helicotrema. This connection is necessary to ensure that the sound waves from the oval window can be transmitted to the whole fluid into the cochlea.

The cochlear duct is filled with endolymph, and it is separated from the tympanic duct by means of the basilar membrane.

Resting on the membrane is the organ of Corti, whose function is to transduce electrochemical signals from sound waves. The Corti contains the so-called hair cells, sensory cells which have a fundamental role in the electro-mechanical transduction. There are two types of hair cells, differentiated by their shape and stereocilia. The inner hair cells detect the sound and transmit it to the brain as a neural signal, through the

deflection of the stereocilia. The outer hair cells are responsible for improving the cochlear frequency selectivity, and have the function of a cochlear acoustic amplifiers.
Upon arrival of the sound waves in the inner ear, the sound vibrations propagate through the fluids, the basilar membrane vibrates, and thousands of hair cells are put in motion. The electrical signal is transmitted to the auditory nerve, to which these sensory cells are connected.
The basilar membrane is not uniform in terms of thickness, and this is what determines its tonotopicity.
This means that different regions of the basilar membrane vibrate in response to different sinusoidal frequencies, based on their different thickness and width.
The width of the membrane increases along its length, from the base to the apex, while the thickness increases from the apex to the base.
The membrane is thus narrowest and most stiff at the base, and this area vibrates at higher frequencies, while it is widest and least stiff at the apex, which is sensitive to the lower frequencies.
This implies that also different hair cells are activated, according to the type of the vibrations in the cochlear fluids, and which regions of the membrane are stimulated. (Prosser and Martini, 2007)

## 1.2 Hearing loss

Hearing loss is a condition where the patient has a partial or total inability to hear sounds.
It can be unilateral or bilateral.
There may be different causes of hearing loss, such as genetic factors, old age, syndromes, trauma, infections, exposure to high levels of noise, birth complications and ototoxicity.
Three main types of hearing loss may be distinguished:

- Conductive hearing loss: this is essentially a mechanical problem for which sound waves cannot get through the outer ear and the middle ear.
- Sensorineural hearing loss: sensory loss is caused by problems in the inner ear (cochlea and other associated structures), neural loss involves the hearing nerve. It is generally permanent and it is the most common type of reported hearing loss (about 90%). Most times this type of hearing loss depends on missing or

damaged hair cells in the cochlea (sensory cells). The hair cells have a central role in the transduction of sound waves into a neural signal.

- Mixed hearing loss: this is a combination of the two previous ones. It is caused by problems in both the outer/middle and inner ear.

Various degrees of hearing loss can be identified, according to the threshold in which the quietest sounds can be detected. These thresholds are expressed in decibels (dB HL). The test to determine the auditory threshold value is carried out over several frequencies, usually 500, 1000, 2000 and 4000 Hz, and the average of the values over these frequencies shall be considered.

- Mild hearing loss: ranges of auditory thresholds between 25 and 40 dB
- Moderate hearing loss: ranges of auditory thresholds between 40 and 70 dB
- Severe hearing loss: ranges of auditory thresholds between 70 and 90 dB
- Profound Hearing loss: auditory threshold above 90 dB.

Finally, it is possible to distinguish between prelingual and post-lingual deafness, on the basis of the time of onset of hearing loss.

The prelingual deafness is generally congenital and it is a kind of hearing loss that appears in infancy and childhood, before the acquisition of language skills. The post-lingual deafness is a hearing impairment which occurs after speech and language skill acquisition. It is generally gradual. (Shearer et al, 2017)

Hearing aids (HA) and cochlear implants (CI) are medical devices used to treat hearing loss.

Hearing aids are used most often, and they are indicated for the treatment of mild to severe hearing loss. They essentially consist of a microphone, which converts sound signals to electrical signals, an amplifier, which increases the signal power, and a speaker, through which the amplified signals are sent to the ear.

Cochlear implants, on the other hand, are implantable devices used if hearing aids are not enough, indicated for patients with severe to profound hearing loss. They are used to reestablish the functions of the cochlea, bypassing the damaged inner ear and electrically stimulating the auditory nerve.

## 1.3 Cochlear Implant

The cochlear Implant (CI) is a medical device that introduces or restores hearing perception in deaf people, with severe to profound hearing loss (> 90 dB HL), who do not receive enough benefit from conventional hearing aids. (Gates and Miyamoto, 2003) The CI procedure may be carried out in both pediatric and adult patients.

### 1.3.1 Technical characteristics

A cochlear implant converts sound energy into electrical signals and stimulates the auditory nerve, bypassing the normal hearing process.
The implant consists of an external removable component, generally sitting behind the ear and an internal component, surgically positioned under the skin, connected to an electrode array located in the cochlea. (Ramsden and Graham, 1995)

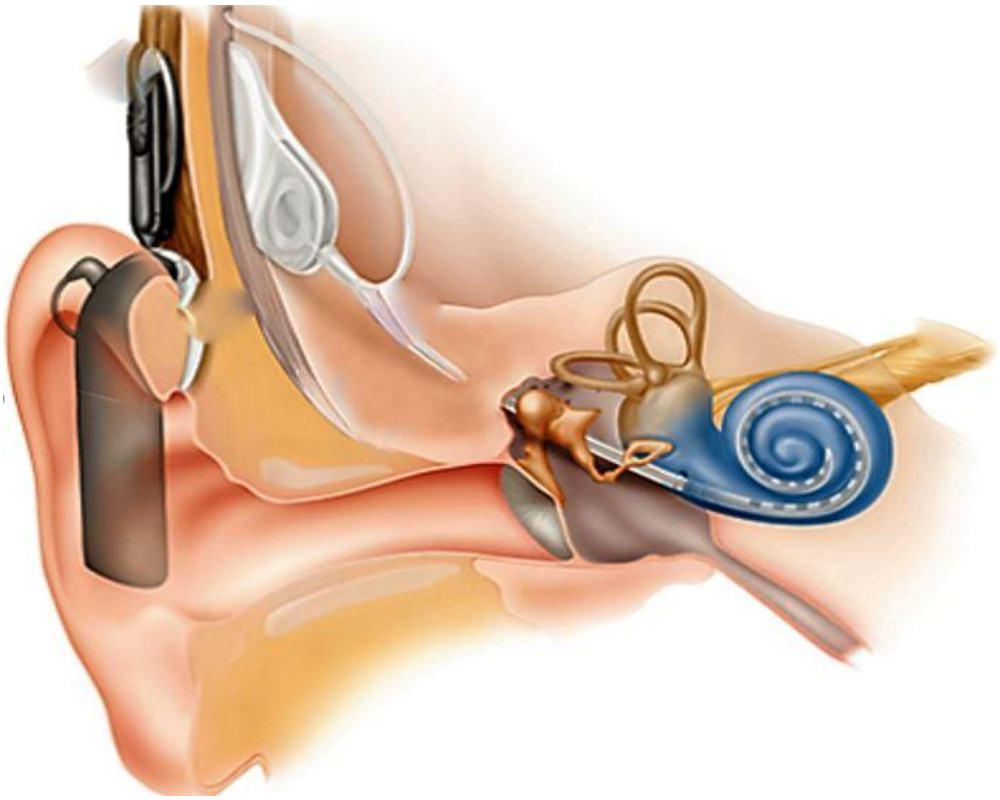

*Figure 1.3.1.1. Cochlear Implant.* https://www.cochlear.com/au/home/understand/hearing-and-hl/hl-treatments/cochlear-implant

The cochlea is characterised by the capability to analyse sounds in both frequency and intensity terms. Specifically, it is differentially sensitive to frequencies.

A sound pressure wave makes the basilar membrane vibrate within the cochlea in the area that is specific to the specific frequency of the vibration. In particular, the base of the cochlea is stimulated by the higher frequencies, and the apex of cochlea by the lower frequencies. This is referred to as cochlear tonotopy.

Therefore, the electrical stimulation of CI electrodes, spaced along the cochlea, allows patients to perceive different sound frequencies, depending on the region where the stimulated electrodes are located.

A normal functioning human ear perceives frequencies in the range from 20 Hz (apical region) to 20 kHz (basal region). A cochlear implant covers the range from 70 Hz to 11.5 kHz. (Dhanasingh and Jolly, 2017)

At present, the electrode array varies from a minimum of 12 electrodes to a maximum of 24, each of which is associated with a specific frequency band.

The external component includes microphones, a digital signal processing (DSP), a battery, an electrical amplifier, and an induction coil for transmitting converted signal through the skin to the inner component of the implant.

The microphones are used to pick up sound from the surrounding environment. The DSP receives them and converts the analogue signal into a digital signal, and then applies signal processing techniques algorithms. The sound is thus encoded into a radio frequency signal, which is then transmitted to the internal component.

Input signal coming in through microphones is filtered into different frequency bands by means of band pass filters.

The transcutaneous link between external and internal component is achieved by means the external antenna and the internal receiver, each with a magnet to provide a magnetic connection.

The external processor is held in place by a magnet attracted to the internal component, located under the skin, behind the ear.

A receiver-stimulator, which contains active electronic circuits, decodes the signal, converts it into electric impulses and sends them to the electrode array along the cochlea. The electrodes stimulate directly the auditory nerve fibres by passing the damaged inner ear. (Zeng and Rebscher, 2009)

The following modes of electrodes stimulation can be distinguished: monopolar, bi- and tri-polar, and common ground stimulation.

Cochlear implants include a feedback system (back telemetry) by which neural electrical activity is monitored. This information is sent to the external component, which in turn is able to monitor the internal component status.

The back telemetry system is essential in ensuring that the internal parts of a cochlear implant perform commands from the external component correctly.

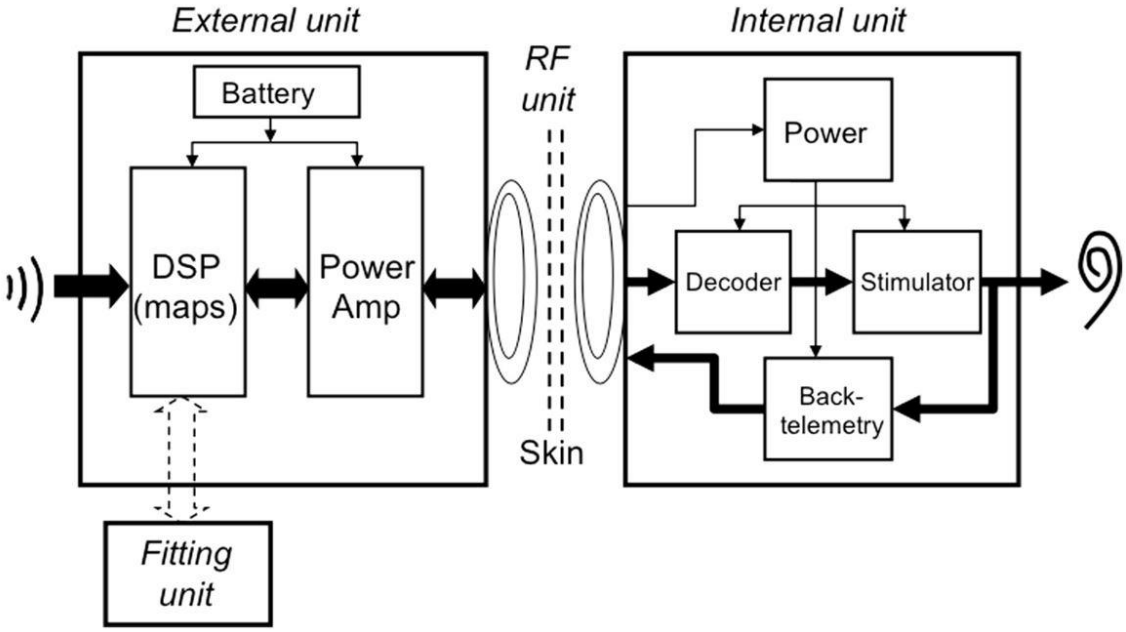


*Figure 1.3.1.2. Cochlear implant functional block diagram.* Zeng FG, Rebscher SJ, Fu QJ. Development and evaluation of the Nurotron 26-electrode cochlear implant system. Hear Res. 2015; 322:188-99.

## 1.3.2 CI activation and follow ups

About a month after surgery, the implant is activated. This activation consists of programming and introducing the external processor. Programming of the speech processor is also defined as mapping. Through the process of CI mapping, the stimulation current levels are set and regulated according to the patient's individual requirements. First fitting and mapping of cochlear implant is performed at this activation stage.

CI maps are therefore individual and editable programs that allow to optimise the implant performances by adjusting the stimulation parameters, such as T and C level.

T level (threshold level) is the minimal electrical stimulation necessary detecting sound, while C level (comfort level) corresponds to the maximum comfortable stimulation.

Both these level are set for each electrode.

After CI activation, regular post-implant follow ups are needed for any maps and other speech processing parameters regulation.

The proper functioning of the external component shall be periodically verified.

Telemetry levels, electrodes impedance and electrophysiological responses should be monitored.

Patients are generally followed up at 1, 3, 6 and 12 months after implant activation, during the first year. After this first period, gradually less frequent follow ups are needed.

CI maps and other information are contained in the memory units of the DPS included in external implant component.

Setting and modifications are performed by means of a specific PC fitting program.

Furthermore, pure tone audiometry and speech audiometry are performed during follow-up, to monitor the level of the auditory threshold. These tests, at the initial phase, allow to determine the degree and type of hearing loss.

Pure Tone Audiometry is an audiological test which makes it possible to identify hearing threshold level. Pure Tone Threshold corresponds to the softest sound audible to a subject, in terms of decibel level. This test is carried out at different frequencies (between 250 Hz and 8000 Hz). Generally, the Pure Tone Average (PTA) is also calculated. It consists of the average of threshold levels at certain frequencies, which are usually 500, 1000, 2000 and 4000 Hz.

Speech audiometry is a test performed in conjunction with pure tone audiometry, that provides information about speech detection, identification and recognition.

### 1.3.3 CI and Magnetic Resonance

Functional magnetic resonance imaging (fMRI) may not be entirely compatible with patients with certain medical devices primarily because of electromagnetic field interactions and artefacts on the MR image.

Compatibility and safety in case of cochlear implantation depends on different CI devices and MRI systems. It should be performed only in case of a precise clinical indication, and according to appropriate safety procedures. (Tang and Li, 2012)

MRI is only partially feasible in patients with cochlear implant due to factors that include a sizable artefact and the risk of the devices being displaced due to potential movement within a magnetic field greater than 1.5 Tesla. (Crane et al, 2010)
A MRI scan with a magnet in place shows a significant amount of shadowing and an artefact at the level of the temporal lobe.

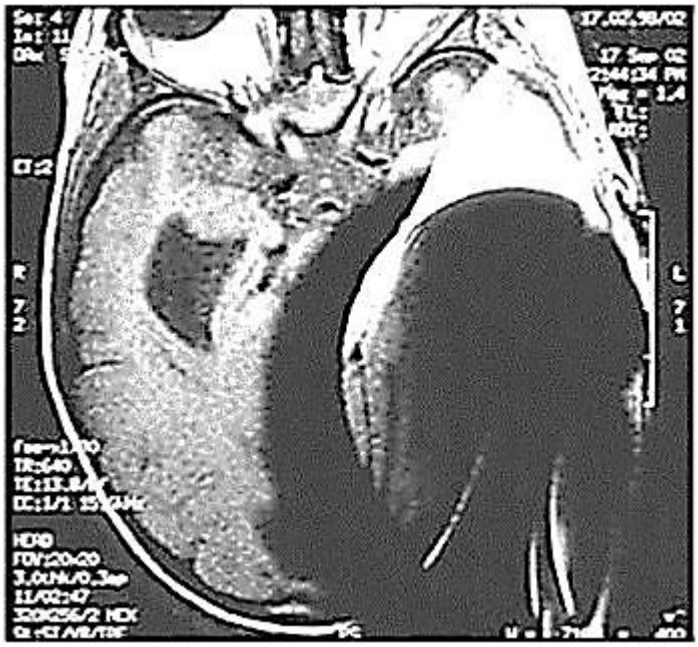

*Figure 1.3.3.1. MRI scan with magnet in place.* F. Risi, A. S. 2004

Imaging artefact can be seen up to 6 centimetres from the cochlear implant, during 3 minutes exposure to a 3 tesla MRI scan, with the magnet removed. And it can be seen up to 12 centimetres from CI during an MRI scan (2 minutes - 0,2 or 1,5 tesla), with the magnet in place.
Moreover, a bandage around the head can be required to prevent possible magnet movement without a removable magnet. But it is not always tolerated by the patient.

## 1.4 Auditory Connectome Model

Many scientific studies agree that early cochlear implantation, in cases of congenital hearing loss, allows patients to develop auditory skills comparable with those of their normally-hearing own age. (May-Mederake, 2012; Niparko et al, 2010)
There is a sensitive period (before three years old), as is well known, for inserting cochlear implant in order to achieve a normal central auditory maturity and properly

develop speech skills. It is the period where the plasticity of the human central auditory system is at its peak. (Sharma et al, 2002; Gordon et al, 2013; Sharma et al, 2005)
However, patients with long periods of profound deafness have worse audiological outcomes compared to subjects implanted at an early stage.
The proper functioning of the auditory processing needs an integration of many types of information, and a synchronised action between the auditory cortex and other cortical and subcortical centres.
This process of integration, and the problem of sensory restoration in early deafness, may be explained by the connectome concept, which is a model of a synaptic network. (Kral et al, 2016)

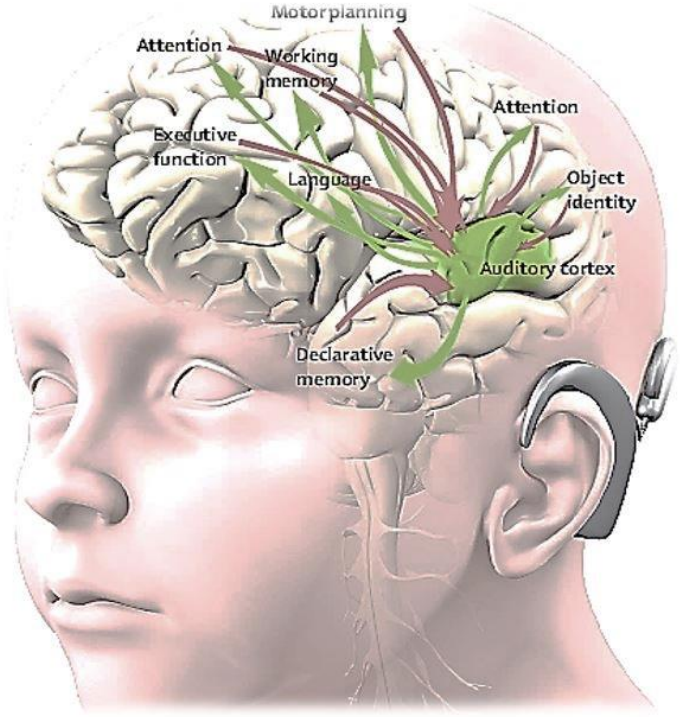


*Figure 1.4.1. "Neurocognitive factors in sensory restoration of early deafness: a connectome model".* Andrej Kral, William G Kronenberger, David B Pisoni, Gerard M O'Donoghue, Lancet Neurol 2016.

The normal development of this neural network depends on sensory experience during the early years of life, and is made impossible by congenital-prelingual deafness.
Connectivity between the auditory system and the high neurocognitive functions relies on both bottom-up (auditory input from periphery) and top-down (auditory cortex modulation from high order areas of the same sensory system or from multisensory areas of the cortex) ways. (Kral et al, 2017)

Absence of the auditory input provokes changes in connectivity “within the auditory system, between sensory systems, and between the auditory system and centres serving higher-order neurocognitive functions”, causing a substantial reduction of the coordinate action between auditory cortex and other cortical and subcortical centres.

Moreover, sensory deprivation in one modality may result in a neural reorganization and development of the remaining sensory modalities (somatosensory cross-modal plasticity).

Auditory input presumably activates a cortical network of higher-order functions and sensory restoration with CI can improve connectivity in this network. (Kral et al, 2016)

A cochlear implant (CI) adds a new auditory modality in deaf patients and improves connectivity in the auditory network model, restoring the auditory connectome.

That implies that prelingual and post-lingual deaf patients with cochlear implants can differ as regards their mechanism of cortical reorganization. In fact, post-lingual deaf patients have a proper process of auditory system development before the onset of deafness, while the same thing does not happen in the case of prelingual deafness. (Stropahla et al, 2017)

In light of these considerations, it may be interesting to study the brain activity of prelingual and post-lingual patients with cochlear implant, in response to auditory stimulation.

# 2. Neurophysiological Analysis

Auditory modality shares with the other sensory modalities the access to superior cortical functions. This complex issue cannot be investigated without a methodology able to depict brain activities such as neuroimaging and neurophysiological techniques. Functional magnetic resonance imaging (fMRI), positron emission tomography (PET), and functional near infrared spectroscopy (fNIRS) might be used.

Changes in cerebral glucose metabolic rate (MRI, PET, fNIRS) and electrical response to auditory stimulation (electroencephalography-EEG) are different effects of auditory stimulation on brain cortical regions.

A cortical activation is associated with an increased brain metabolism. (Crosson et al, 2010)

Spatial patterns of cortical activation may be evaluated using functional MRI.

MRI makes it possible to examine the haemodynamic response associated to brain activity, and it has a good spatial (3-6 mm) and a low temporal resolution (1-2 s). Magnetic fields, radio waves and field gradients are used to form MRI images. This procedure should be carried out only in case of a precise clinical indication, according to specific safety precautions, since it is a method only partially compatible with cochlear implants. (Tang and Li, 2012)

PET is another technique used to evaluate brain activity through analysis of metabolic changes. It has a poor temporal resolution, and it has a spatial resolution worse than fMRI. It is a method which uses properties of short half-lives of most positron-emitting radioisotopes to map brain systems responsible for cognition. It provides a measure of cerebral blood flow by analysing the direct relationship between high radioactivity and brain activity, from a neurological standpoint.

Metabolic changes can be measured near the brain surface by means of NIRS technique. It monitors the levels of local oxyhemoglobin and deoxy-haemoglobin concentrations related to cerebral activation to evaluate brain activity, by measuring the optical absorption coefficients.

This method has a better time resolution compared to fMRI (ms). However, it does not have a good spatial resolution (accuracy within the range of cm).

A different functional brain imaging method consists of Electroencephalography (EEG). Despite a poor spatial resolution, which can be improved by increasing the number of recording electrodes, this technique has an excellent time resolution and it is perfectly

compatible with cochlear implants. EEG allows estimation of cortical activation even at sub-second timescales.

EEG provides a measure of the basal brain electrical activity, but if brain response to specific sensory stimulation is to be achieved, Event-Related Potentials (ERPs) should be recorded.

In a second step, cortical sources of signal can be estimated using a low resolution tomography. This type of analysis could therefore be a very appropriate method to investigate auditory system in patients with cochlear implant, from a sensory and neurocognitive perspective.

## 2.1 EEG

Electroencephalography is an electrophysiological technique that allows recording of brain electrical activity, more specifically, differences in electrical potential.

The synchronized neural activity is recorded at a very high temporal resolution by means of a number of electrodes placed on the scalp.

This voltage distribution on the scalp is generated from the neural currents by the post-synaptic potentials in the apical dendrites of pyramidal neurons inside the brain. (He et al, 2011)

These are neuronal cells located in the cerebral cortex, characterized by a pyramidal shaped soma, a large apical dendrite, multiple basal dendrites, and a single axon. They project axons to other cerebral regions, and to the spinal cord.

Pyramidal neurons can be excited by the neurotransmitter glutamate and they can be inhibited by the GABA receptors. (Megías et al, 2001)

Important features of this type of cells are their axonal and dendritic branching, that allow them to receive and send signals to and from a great number of neurons, and their orientation, aligned perpendicularly to the cortex surface.

Their capacity to integrate information is related to the numbers of the synaptic inputs received from other cells. A pyramidal neuron can receive about thirty thousand excitatory inputs.

Just like other nervous system cells, they have a large number of ion channels. Voltage-gated calcium ion channels in cell dendrites are activated by excitatory postsynaptic and back propagating potentials. The amplitude of action potential is controlled by a mechanism provided by potassium channels. (Barnett and Larkman, 2007)

Synaptic inputs to a neuron cause plasma membrane depolarization or hyperpolarization. An action potential is triggered due to the synaptic inputs arrival at cell dendrites, when the value of depolarization is sufficient to exceed the threshold value.

The action potential spreads through the pyramidal neuron, and that leads to a ionic movement which gives rise to an electric dipole (a pair of electric charges of opposite sign, characterized by magnitude and direction).

Specifically, axonal action potential causes a depolarization of the dendritic membrane, which is associated with extracellular electronegativity in the apical zone and with electropositivity in the basal zone. So, an extracellular current flows from positive to negative. Simultaneously, an intracellular current flows into the dendrite in the opposite direction. A balance of charge is provided inside the cell by the extracellular charge flow in about 10-40 ms.

In this sense it is possible to say that the electric potential generated by neuronal cells may be modelled by a dipole.

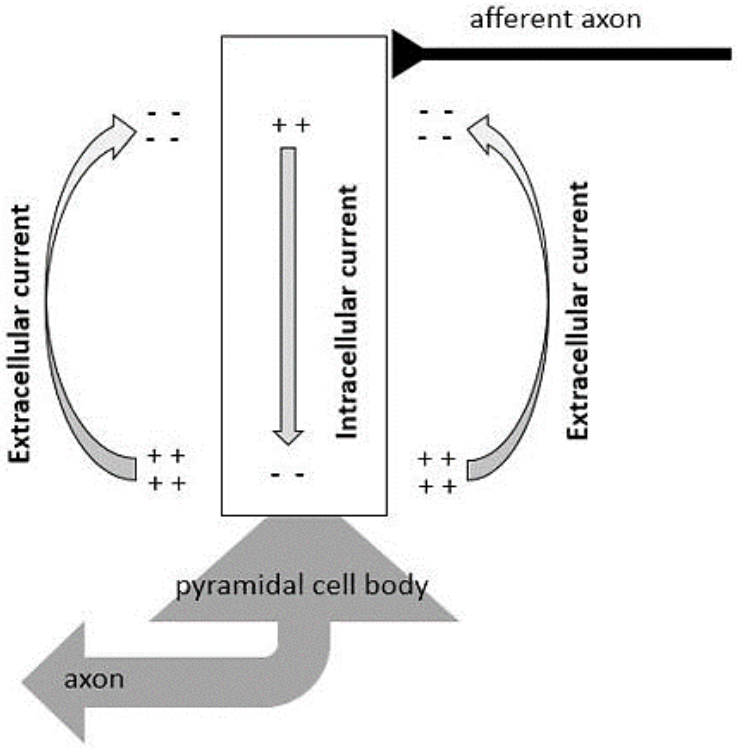


*Figure 2.1.1. Dipolar current flow in a pyramidal neuron*

The distance between the two charges is much smaller than the distance of the recording electrode from the electrical activity source.

Furthermore, the electric field strength of the dipole is too small to be measurable by an EEG electrode.

So, a great number of pyramidal neurons need to be activated at or near the same time, so that the equivalent dipole can be recorded by an electrode. It is estimated that around 50.000 cells are necessary. (Lopes da Silva, 2010)

This means that about 50.000 simultaneously active pyramidal neurons give rise to a measurable electroencephalographic signal.

It is the specific and non-specific thalamo cortical projections that make a synchronization of cortical activity possible.

The potential produced by the dipole and recorded by the electrodes is directly proportional to the magnitude of charge q, to the cosine of the θ (angle between the dipole axis z and the distance r between the dipole centre and the electrode position), and to the distance between charges. Instead, it is inversely proportional to the square of r and to the electric constant $\varepsilon_0$.

$$V = \frac{qd\cos\theta}{4\pi\varepsilon_0 r^2}$$

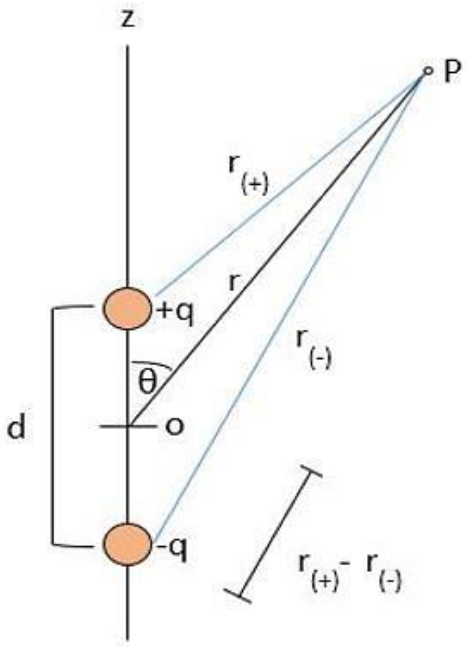


*Figure 2.1.2. Diagram of electric dipole aligned along z axis.*

The radial component of the dipole can be correctly detected by the electroencephalography technique (θ=0 and cosθ=1), while no potential is detected from tangential components (θ=90 and cosθ=0).
Therefore, the measured potential becomes smaller as the distance between cortical source and electrode is increased.

EEG rhythms

Cortical activity consists globally in the whole group of electrical equivalent dipoles. It is characterized by waveforms of different amplitudes and frequencies.
The amplitude of EEG waves depends on the level of synchronization by which pyramidal neurons interact with each other. An asynchronous electrical excitation generates a low amplitude and irregular signal, while a neuronal cells synchronization generates a high amplitude signal, resulting from the sum of all single cellular electrical activity.
In any case, human eeg rhythms have quite a small intensity, measured microvolt (μV), from 10 to 100 μV, and in terms of their spectral content, different eeg frequency bands are distinguished: δ, θ, α, β.

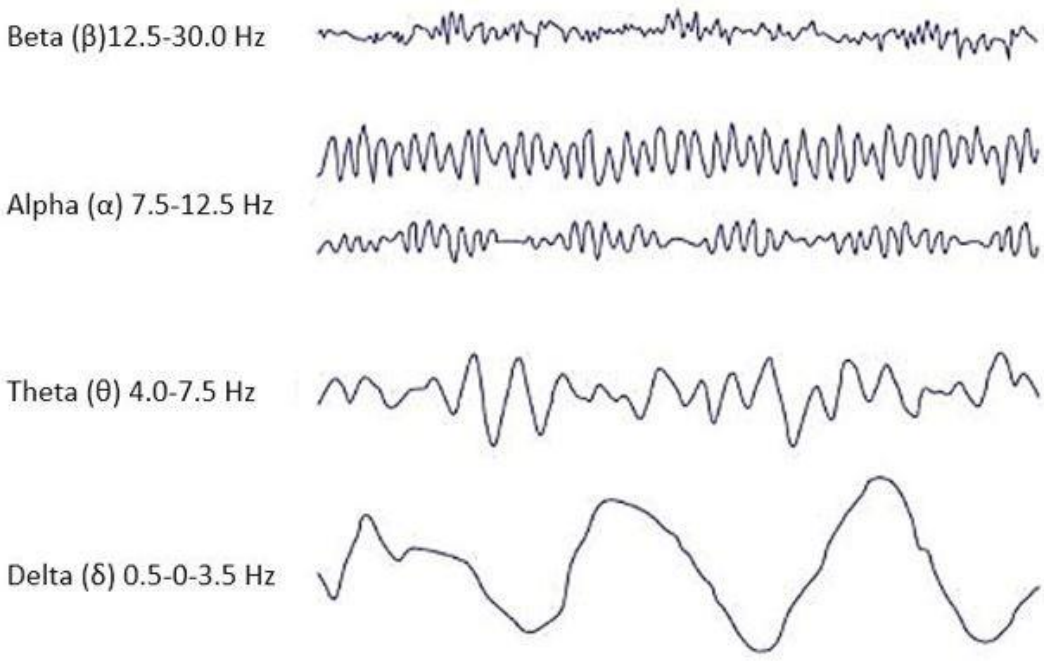


*Figure 2.1.3. Human EEG rhythms.* Tye C, McLoughlin G, Kuntsi J, Asherson P. Electrophysiological markers of genetic risk for attention deficit hyperactivity disorder, 2011.

- Delta rhythm: frequency between 0.5 and 3.5 Hz. Generally, the highest rhythm in amplitude and slowest waves. Normally in babies up to one year old, in adults during stages 3 and 4 of sleep. This rhythm predominantly occurs in frontal areas (adult people) and posterior regions (children).
- Theta rhythm: frequency between 3.5 and 7.5 Hz. Classified as slow activity, it normally occurs in children up to 13 years old and during sleep, while it is pathological in awake adult people. It is usually associated with the temporal brain areas.
- Alpha rhythm: frequency between 7.5 and 12.5 Hz. It is usually most prominent in the temporo-parietal-occipital regions. It occurs when subjects close their eyes, and during the resting state. It is the more visible rhythm in health and relaxed adult. It is then subdivided into two rhythms: alpha 1 (8-10 Hz) and alpha 2 (10-13 Hz).
- Beta rhythm: frequency between 12.5 and 30 Hz, classified as fast activity. It is usually seen at level of frontal regions. It is the rhythm that mainly occurs in adults during the alert or anxiety state.

Time and Frequency domain

It is extremely important to be able to analyse the EEG signals both in terms of temporal and spectral features.

Time domain analysis consists of evaluating the variation of amplitude of EEG signal with time. Therefore, time domain features are amplitude related (energy, periodicity, mean, variability). This type of analysis may also provide information on the synchronization of different EEG signals, by measurement of phase shift and phase lock.

Time domain analysis can provide excellent spatial information, but it does not provide any indication of signal frequency content.

Frequency domain analysis makes it possible to determine the frequency components of a signal and estimate all related features in frequency, the most assessed of which is Power Spectral Density (PSD). This estimates the amount of power at each frequency.

The Fourier transform (FT) is the most common mathematical method for calculating frequency components in EEG signal. FT decomposes the EEG signal into its different frequencies, allowing separation of different EEG rhythms. (Harpale and Bairagi, 2016)

For a given function f(x) in the time domain, where x is a measure of time, the Fourier transform is defined by:

$$F(\omega) = F\big(f(x)\big)(\omega) = \int_{-\infty}^{\infty} f(x)e^{-i\omega x}dx$$

function in the frequency domain, (ω).

The inverse transform, however, is defined by the following expression:

$$F^{-1}(F(\omega))\,(x) = \frac{1}{2\pi}\int_{-\infty}^{\infty} F(\omega)e^{i\omega x}d\omega$$

EEG recording

In conventional EEG recording, a certain number of electrodes are placed on the scalp in specified positions, according to the International 10/20 system.

The "10/20" name is due to the fact that the effective distances between two adjacent electrodes are either 10% or 20% of the whole distance from the nasion to the inion or the whole distance from both preauricular areas.

Each electrode position is characterized by a letter, which refers to the corresponding underlying area of cerebral cortex (Pf=prefrontal, F=frontal, T=temporal, P=parietal, O=occipital, C=central), and a number, that identifies the hemisphere: even numbers on the left side, odd numbers on the right. There are also a few electrodes identified by means of addition of the letter "Z", and they are the electrodes placed on the midline sagittal plane of the scalp.

In this way, EEG electrodes positioning may be standardized.

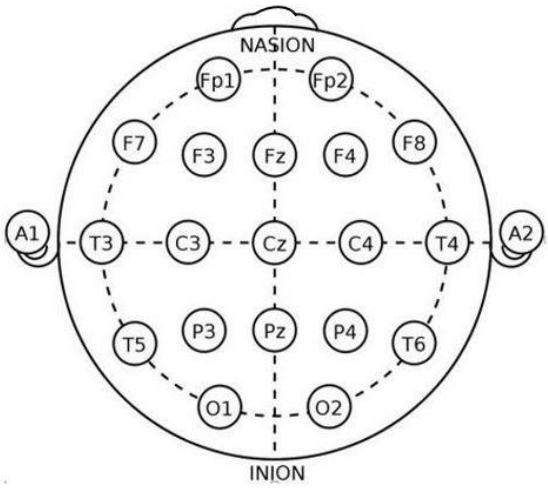


*Figure 2.1.4. International System 10-20*

A distinction can be made between monopolar (or referential) and bipolar montage. The monopolar mode consists of recording EEG potential as potential difference between each electrode and a designed reference, while a potential difference between adjacent electrodes is recorded in the bipolar mode.
EEG signal is quite small, measured in microvolts, and it may be affected by different types of artefacts, so it needs to be amplified and filtered.
The noise artefact caused by recording electrodes can be reduced by means of differential amplifiers, each connected to one electrode.
A low pass filter makes it possible to reject noise and any artefacts at high frequencies.
A high pass filter allows a reduction of the effect of the voltage from the galvanic skin response across the head.
A notch filter is used to reject a specific frequency (typically 60 or 50 Hz). It is a very selective filter that can reject just a small frequency band around the selected frequency, while leaving the rest of the spectrum basically unchanged.
Evoked potentials evaluation and EEG spectral content analysis are two of the most common EEG diagnostic application.

### 2.1.1 Auditory Evoked Potentials

Evoked potentials (EPs) are scalp-measured voltage fluctuations, generated in response to a specific event. They are changes in the brain's electrical activity, time locked to a sensory, motor or cognitive event.
Each EP wave represents a sum of potentials elicited in widely distributed cortical sources. (Kropotov, 2016)
Two types of EPs can be identified:

- Stimulus related potentials: exogenous potentials generated by external stimulation. They allow an objective measure of the functions of the sensory systems to be obtained.
- Event related potentials: endogenous potentials which do not only involve a simple stimulus response, but are associated with cognitive related neural activity.

It is possible to distinguish three EPs categories, based also on their latency:

- Short latency evoked potentials: latency <30 ms

- Middle latency evoked potentials: latency 30-75 ms
- Long latency evoked potentials: latency >75 ms.

Signal averaging technique

EPs are usually smaller than the EEG signal.

Their low amplitude, in the range of 0.1-10 μV, makes them difficult to be clearly distinguished from the background EEG activity (about 10-100 μV when measured on the scalp).

The voltage measured by the electrode v(t) consists of the algebraic sum of the following elements:

s(t): the potential evoked by stimulation, needed to be evaluated.

n(t): the whole group of potentials which do not just relate to the stimulus, noise which shall be minimised.

$$v(t) = s(t) + n(t)$$

A signal processing technique called averaging shall be used in the time domain, in order to maximise the signal and minimise the noise (which in this case is the background EEG activity).

Neural networks generate a constant evoked potential in the replicate measurements:

$$s_1(t) = s_2(t) = \ldots = s_m(t)$$

This signal is uncorrelated to noise.

Instead, the background EEG activity is random, uncorrelated, with a mean of zero and constant variance in the replicate measurements.

So the reliable EP is obtained by averaging EEG fragments in multiple trials.

$$\frac{1}{m}\sum_{i=1}^{m} v_i(t) = \frac{1}{m}\sum_{i=1}^{m} s_i(t) + \frac{1}{m}\sum_{i=1}^{m} n_i(t) = \frac{1}{m}\sum_{i=1}^{m} s_i(t) = \frac{1}{m} ms(t) = s(t)$$

(m = number of trials).

Being $\lim_{m\to\infty} \frac{1}{m}\sum_{i=1}^{m} n_i(t) = 0$

As is known, the signal-to-noise ratio (s/n) increases in proportion to the square root of m, which is therefore a key parameter in the EPs recording.

The number of trials required in average depends on the amplitude of the background activity.

Event related potentials (ERPs)

As stated above, ERPs are EEG changes elicited by sensory, motor or cognitive events. (Sur and Sinha, 2009)

Using event-related potentials (ERPs), the neural correlates of cognitive processes can be investigated non-invasively.

A key advantage of ERP methods is that they provide measures of neural activity with very high temporal resolution. The superior temporal resolution of ERPs makes them well suited to examine neural events responsible for cognitive tasks, which can potentially be monitored by ERPs on a millisecond-by-millisecond basis.

There are early waves, elicited within the first 100 ms after stimulus, and late waves, elicited from 100 ms after stimulus.

Among the late waves N100, N200 and P300 waves are included.

- N100: is a negative potential, observable between 80 and 200 ms after the onset of stimulus, in absence of cognitive task by the subject. It is essentially related to stimulus perception.
- P200: is a negative deflection that peaks around 200 ms after the onset of stimulus. It can be considered an index of a cognitive process of stimulus identification and discrimination.
- P300: is a positive deflection generated between 250 and 400 ms after the onset of stimulus. This wave is one of the late auditory event related potentials, elicited in the process of decision-making. It reflects the cortical processes involved in stimulus evaluation and categorization, during attention, discrimination of one stimulus from another, memory operations, integration and decision-making skills. (Reis, et al 2015)

Auditory evoked potentials (AEPs)

Evoked potentials are carried out to examine the integrity of peripheral and central neural conduction pathways. Auditory evoked potentials, in particular, provide information about neural activity deriving from structures ranging from the auditory nerve to the cortex.

Long latency auditory evoked potentials (LLAEP) can be used to evaluate neurophysiological changes that compromise the cortical regions of the auditory pathway, in terms of skills of cognitive elaboration. (Perez et al, 2017)

Auditory P300 is an objective measurement of cognitive processes induced by auditory stimulation. Therefore, the recording of P300 may be useful for the study of the auditory system and the higher neurocognitive functions associated with it, also in patients with cochlear implant.

P300 is generally elicited using the oddball paradigm.

The active oddball paradigm consists of a task in which stimuli are presented in a continuous sequence and participants must identify the presence of target stimuli and keep count of them. These stimuli occur randomly, and infrequently compared to other standard stimuli, and have different characteristics (e.g. a different tone).

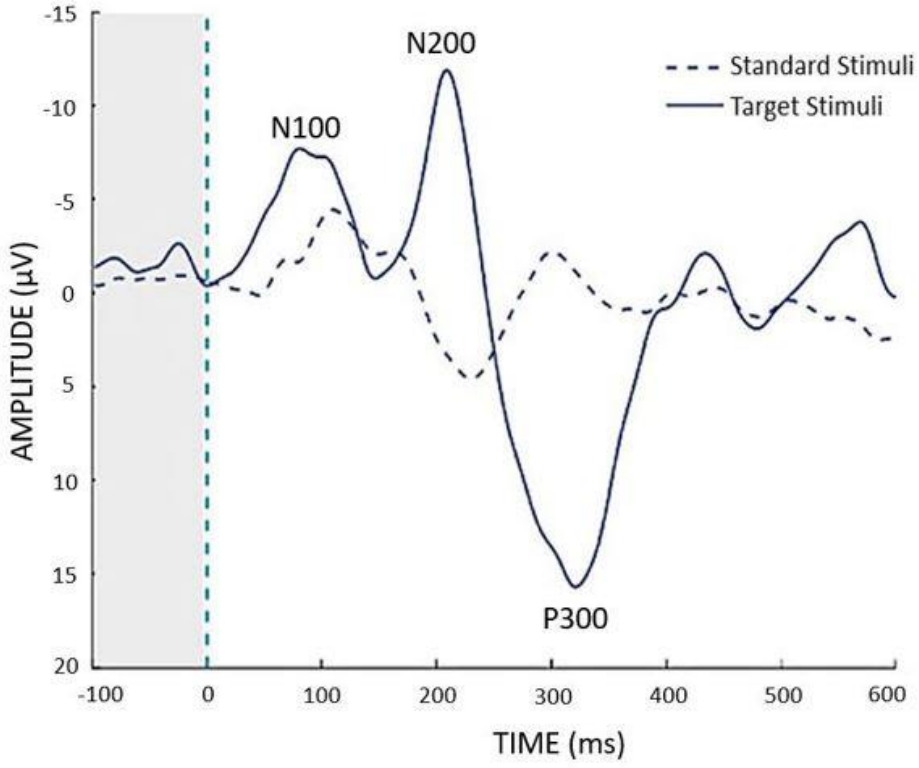


*Figure 2.1.1.1. Long latency auditory evoked potentials (LLAEP)*

## 2.2 EEG Inverse Problem

Event-related potentials (ERPs) are generally evaluated through latency and amplitude values. However, this kind of analysis is not enough in a study of processing in cerebral auditory cortex. Cortical activation pattern during Erps elicitation must be analysed.

The cortical source estimation from electroencephalographic recordings represents an inverse problem, because it is about determining, from a set of measures, the causal factors that produced them. The inverse problem in EEG source localization, therefore, consists of finding the electrical sources which generate a measured brain signal. (Grech et al, 2008)

This is a highly underdetermined problem, because the number of recorded measures (equal to the number of electrodes) is lower than the number of unknown variables (cortical current sources). So, there is not a unique solution, and it is more accurate to say that there is a probability of sources distribution describing the neural current distribution. So, the one which is determined, is an approximate solution.

Neural activity can be modelled by current density, whose source locations can be well approximated by current dipoles, defined by position, orientation and amplitude.

The method of resolving this problem is to take measures of the voltage potential at various locations on the scalp, and then use specific software to estimate the current brain sources that best fit the acquired data. (Grech et al, 2008)

### 2.2.1 LORETA

Low-resolution brain electromagnetic tomography (LORETA) is a functional imaging technique that allows estimates of cortical sources of EEG signal, providing a solution of the EEG inverse problem.

The EEG signal is a recording of electrical potential differences, and Loreta software is able to detect the relative neural activity of brain regions using surface electrodes and estimating current densities at a deeper cortical level. (Pascual-Marqui et al, 2002)

This is a reference-free method of EEG analysis, as it does not depend on the reference electrode used in recording the eeg signals.

Brain electrical activity can be detected in all cortical structures by means of registering the solution space to a brain atlas.

The software calculates linear 3D solutions, by means of a brain compartment model consisting of 6239 voxels with resolution of 5 mm (the initial version included 2394

voxels with a spatial resolution of 7 mm), each one being associated with an equivalent current dipole of EEG activity. Each Brodmann Areas is modelled by a certain number of voxels.

Loreta implements a three-shell spherical head model (skin, skull, and cortex), which is co-registered to the MRI atlas of Talairach and Tournoux. (Pascual-Marqui et al, 1994)

The brain compartment is restricted to the cortical grey matter-hippocampus of a head model co-registered to the Talairach probability brain atlas. (Talairach and Tournoux 1988)

A voxel was classified as grey matter if its probability of being grey matter exceeded 33%, exceeded the probability of being white matter, and exceeded the probability of being cerebrospinal fluid. (Pascual-Marqui, 2002)

Cross-registrations between spherical and realistic head geometry are used to obtain EEG electrodes coordinates. (Towle et al, 1993)

The following table shows the distribution of voxels in the different Brodmann Areas:

| BA | Area Names | Left Side | Right Side | Center | |
|---|---|---|---|---|---|
| 1 | Primary Somatosensory Cortex | 9 | 9 | 0 | |
| 2 | Primary Somatosensory Cortex | 43 | 49 | 0 | |
| 3 | Primary Somatosensory Cortex | 72 | 72 | 0 | |
| 4 | Primary Motor Cortex | 69 | 64 | 1 | |
| 5 | Somatosensory Association Cortex | 40 | 41 | 9 | |
| 6 | Premotor cortex | 263 | 274 | 13 | |
| 7 | Somatosensory Association Cortex | 186 | 183 | 25 | |
| 8 | Frontal eye fields | 74 | 89 | 9 | |
| 9 | Dorsolateral prefrontal cortex | 124 | 135 | 9 | |
| 10 | Anterior prefrontal cortex | 136 | 134 | 2 | |
| 11 | Orbitofrontal area | 115 | 122 | 0 | |
| 13 | Insular cortex | 125 | 117 | 0 | |
| 17 | Primary visual cortex | 36 | 39 | 2 | |
| 18 | Secondary visual cortex | 145 | 143 | 28 | |
| 19 | Associative visual cortex | 186 | 179 | 2 | |
| 20 | Inferior temporal gyrus | 109 | 112 | 0 | |
| 21 | Middle temporal gyrus | 105 | 125 | 0 | |
| 22 | Superior temporal gyrus | 88 | 93 | 0 | |
| 23 | Ventral posterior cingulate cortex | 15 | 18 | 15 | |
| 24 | Ventral anterior cingulate cortex | 61 | 69 | 20 | |
| 25 | Ventromedial prefrontal cortex | 16 | 19 | 8 | |
| 27 | Piriform cortex | 7 | 9 | 0 | |
| 28 | Ventral entorhinal cortex | 21 | 20 | 0 | |
| 29 | Retrosplenial cingulate cortex | 5 | 4 | 0 | |
| 30 | Part of cingulate cortex | 37 | 37 | 3 | |
| 31 | Dorsal Posterior cingulate cortex | 80 | 90 | 29 | |
| 32 | Dorsal anterior cingulate cortex | 70 | 76 | 10 | |
| 33 | Dorsal anterior cingulate cortex | 2 | 3 | 2 | |
| 34 | Dorsal entorhinal cortex | 17 | 16 | 0 | |
| 35 | Perirhinal cortex | 13 | 13 | 0 | |
| 36 | Ectorhinal area | 30 | 26 | 0 | |
| 37 | Fusiform gyrus | 96 | 91 | 0 | |
| 38 | Temporopolar area | 76 | 88 | 0 | |
| 39 | Angular gyrus | 77 | 64 | 0 | |
| 40 | Supramarginal gyrus | 189 | 188 | 0 | |
| 41 | Auditory cortex | 27 | 28 | 0 | |
| 42 | Auditory cortex | 19 | 20 | 0 | |
| 43 | Primary gustatory cortex | 14 | 12 | 0 | |
| 44 | Pars opercularis | 28 | 28 | 0 | |
| 45 | Pars triangularis | 29 | 34 | 0 | |
| 46 | Dorsolateral prefrontal cortex | 20 | 25 | 0 | |
| 47 | Inferior frontal gyrus | 107 | 113 | 0 | |
| | | | | | **Total voxels** |
| | | 2981 | 3071 | 187 | **6239** |

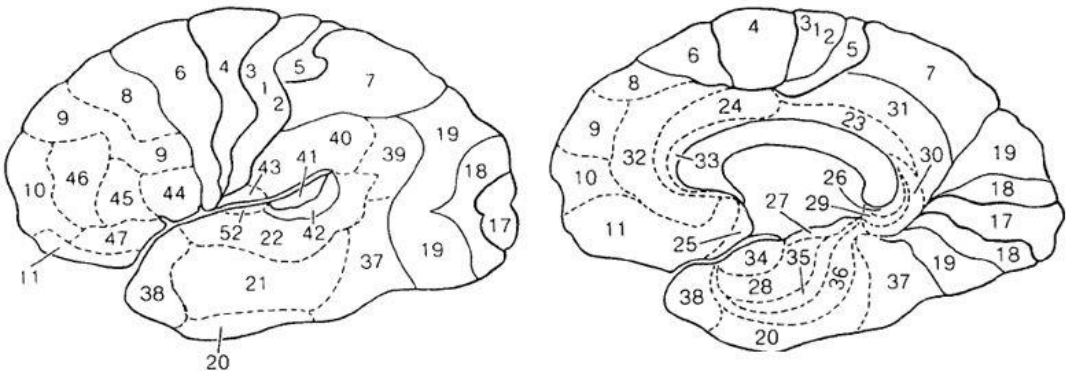


*Figure 2.2.1.1. Brodmann's areas of the cortex.* Textbook of Neuroanatomy. H. Chandler Elliott. Lippincott, Philadelphia.

As it is an underdetermined problem, LORETA cortical solutions have been structured to estimate distributed rather than punctual EEG source patterns.

To ensure that Loreta can accurately solve the linear inverse problem, some assumptions must be considered. Neurons that are next to each other are assumed to be fired synchronously and all at the same time, and the solution is determined on a basis of maximal smoothness, as the software consider the brain active dipole configuration which minimizes the squared norm of the Laplacian of the weighted 3D current-density vector field.

In this way, the localization of cortical sources, even the deepest ones, can be obtained correctly, and the software can prevent any possible effects of spatial aliasing of the source solutions. (Pascual-Marqui, 1994; Babiloni et al, 2015)

Loreta can determine the current densities in each of the 6239 voxels of grey matter, from recorded values of EEG potentials, by calculating the three Cartesian components of each vector.

This standardized brain electrical activity can also be visualized by means of different kinds of cerebral images reconstructed by the software.

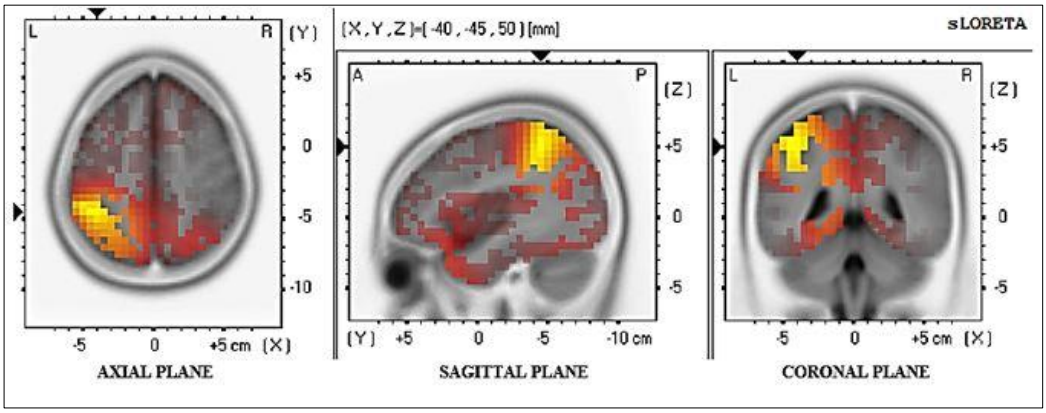


*Figure 2.2.1.2. Loreta probabilistic map in cortical difference of activation – Slice-Viewer*

*Figure 2.2.1.3. Loreta Viewer - 3D Cortex Activation*

In order to perform statistical analysis, a specific function is provided by the software. This makes it possible to perform the t-test with several options and display the results in statistical parametric maps, taking into account the multiple statistical measurements (5000 randomizations are performed).

Loreta software can be used in both time and frequency domain. It is possible to calculate the eeg signal sources and the sources of the eeg frequency components respectively.

Functional dynamic brain connectivity, quantified by coherence and phase synchronization, can be evaluated between all pairs of ROIs (region of interest) by using the lagged phase synchronization method.

This method allows the evaluation of similarity between signals in the frequency domain.

EEG signals or EEG tomography, however, may include artefacts, such as volume conduction effect and non-physiological components. For this reason, lagged connectivity measures must be adjusted by means specific corrections, to ensure that lagged phase synchronization include only physiological connectivity information. (Pascual-Marqui et al, 2011)

**Functional brain connectivity**

Functional brain connectivity can be analysed in both frequency and time domain.

Brain connectivity, analysed by signal processing in the time domain, is the connectivity between different cerebral areas which share functional properties.

This kind of analysis is carried out by the investigation of the changes in cerebral blood flow and in cerebral glucose metabolism. Neuroimaging techniques and methods such as correlation and granger causality are generally used for this purpose.

An analysis of cerebral perfusion and metabolism can allow to identify which brain areas are most active during a specific process, which areas are similar from a metabolic point of view, and so which areas are functionally linked.

However, this kind of analysis gives no specific information about whether these areas also appear linked when compared in terms of frequency bands.

A connectivity model associated with the frequency domain can be used for this type of analysis, and the assessment is carried out using methods such as coherence and phase synchrony.

These are mathematical methods which make it possible to evaluate frequency and phase dependent correlations of brain activity.

Functional connectivity analysis does not consider anatomical observations and metabolic processes. This type of analysis is based on brain signal content estimation. Brain areas which have similar signal content and are most functionally connected.

In this case the question is whether there is a coherence between the different brain areas.

The human brain can be described as a network model in which a large number of neural pathways are connected by a synchronized electric brain activity. It is possible to detect this synchronized activity by means of connectivity analysis on Electroencephalography (EEG), Magnetoencephalography (MEG) and Functional Magnetic Resonance imaging (fMRI) data. (Bowyer, 2016)

So, when referring to functional connectivity, the relationship between spatially separated brain regions that have similar frequency, phase or amplitude of correlated activity is meant.

These correlated brain areas may be involved during the resting state, when any kind of specific task is not being performed, or during higher order information processing.

In this study an analysis of functional connectivity using the coherence method was performed on EEG data.

The coherence method makes it possible to evaluate if different brain regions are generating significantly correlated signals or not.

From a mathematical perspective this method determines the neuronal patterns of synchronicity, quantifying frequency and amplitude parameters on the basis of EEG data recorded on scalp electrodes.

This means that coherence shall provide an estimation of the consistency of amplitude and phase between electroencephalographic signals from surface electrodes, in relation to specific different frequency bands. (Bowyer, 2016)

In statistics, correlation is a mathematical method that can determine if a pair of variables (x and y, for example) are related, and eventually how strong this relation is.

Correlation is a measure of how these variables covary with respect to each other and depend on the other.

If the first variable can be written as a linear function of the second, the two variables are linearly dependent, and it can be defined as linear correlation.

The two variables x and y are said to be positively linearly correlated when y increases with increasing x. Therefore, correlation is negative when y value decreases if x value increases.

The correlation between variables x and y can be expressed as $r_{xy}$ (Pearson correlation coefficient), and its value can vary between -1 and +1, where 1 is correspondent to the perfect positive correlation, -1 to a perfect negative correlation, and 0 value represents no correlation between the two variables.

The formula for r is:

$$r_{xy} = \frac{cov_{xy}}{\sqrt{\rho_x \rho_y}}$$

($cov_{xy}$ is the covariance between x and y, $\rho_x$ is the standard deviation of x variable and $\rho_y$ is the standard deviation of y).

This measure does not include the cause-effect relationship; it reveals only a systematic correlation between variables.

Correlation between different brain regions, calculated in relation to specific frequency bands, should be considered when it comes to signals analysis. In this sense, the concept of coherence can be introduced.

It is basically a "frequency-correlation", it can be considered as a sort of spectral version of correlation. (Peraza et al, 2012)

From a mathematical point of view, every periodic signal may be deconstructed into a series of sine or cosine terms (imaginary and real part of the function), defined as Fourier series. Each of these terms of the series has specific coefficients related to signal amplitude and phase.

The formula for f(x) function, integrable on an interval [-h, h], is:

$$f(x) = \frac{a_0}{2} + \sum_{n=1}^{\infty} a_n cos\frac{\pi nx}{h} + b_n sin\frac{\pi nx}{h}$$

$$\begin{cases} a_n = \frac{1}{h}\int_{-h}^{h} f(x) cos\frac{\pi nx}{h} dx \\ b_n = \frac{1}{h}\int_{-h}^{h} f(x) sen\frac{\pi nx}{h} dx \\ a_0 = \frac{1}{h}\int_{-h}^{h} f(x) dx \end{cases}$$

Coherence is defined as:

$$r_{xy}(\lambda) = \frac{|f_{xy}(\lambda)|^2}{f_{xx}(\lambda) f_{yy}(\lambda)}$$

($f_{xy}(\lambda)$ is the cross spectrum between x and y time signals, and λ is the frequency index). (Peraza et al, 2012)

EEG volume conduction problem

In the case of coherence analysis on EEG data, the volume conduction problem must be taken into consideration.

When recording an electroencephalographic signal, a linear correlation between the simultaneously EEG registrations may appear only due to the conductive properties of the volume through which signals are propagated.

And that is because when a signal generated by a specific cortical source spreads, other brain regions are also involved. So, all the regions would be correlated between them,

and a recorded signal might not be necessarily generated by a cortical source below it. (Peraza et al, 2012)

Volume conduction phenomenon causes an instant and phaseless correlation (zero lag) between all cortical sources, and in this sense might affect the synchronization measures.

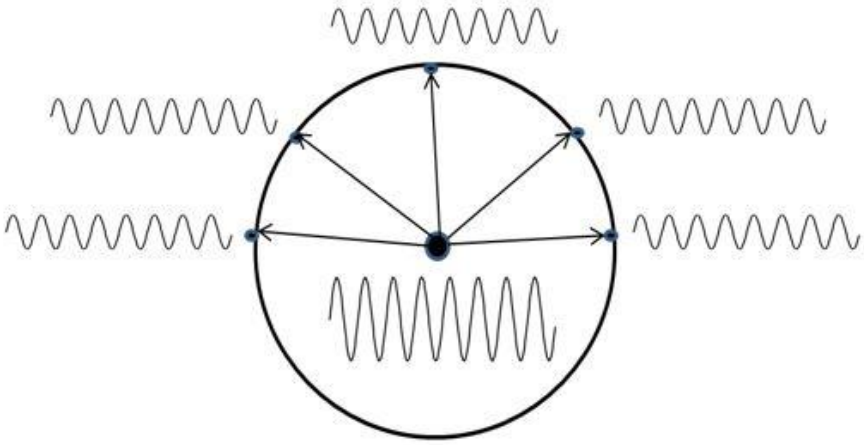

*Figure 2.2.1.4. Sinusoidal wave generator – 8 Hz. No phasing for volume conduction only (lag=0).*

However, if cortical networks are interposed between the signal generator and measuring points, then this is a signal phasing.

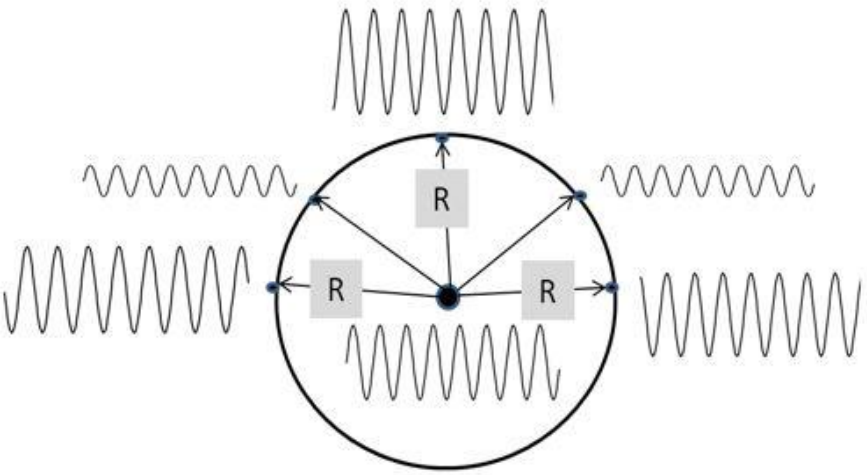


*Figure 2.2.1.5. Sinusoidal wave generator – 8 Hz, with interposed cortical networks. Various degrees of signal phasing (lag≠0).*

It is therefore important to use an instrument able to identify phasing (lag≠0) frequency correlation. By acting in this way, we can exclude any measure due to only volume conduction.

Coherence analysis and Loreta software

Loreta software can be used in frequency domain for evaluating functional dynamic brain connectivity, quantified by coherence and phase synchronization. (Grech et al, 2008)

Functional connectivity between all pairs of ROIs (region of interest) can be analysed by using the lagged phase synchronization method. This method allows the assessment of similarity between signals in the frequency domain.

EEG signals or EEG tomography, however, may include artefacts (for example volume conduction effect), and non-physiological components. For this reason, lagged connectivity measures must be adjusted by means specific corrections, to ensure that lagged phase synchronization include only physiological connectivity information.

Since the first publication about Loreta in 1994, significant improvements have been made in the method. The software was implemented by Pascual-Marqui in 2002, and it was named sLoreta (Standardized low resolution brain electromagnetic tomography). Compared to the previous version, sLoreta has the benefit of detecting cortical sources with zero localization error in the absence of noise. sLoreta is the only linear tomography technique with this characteristic.

A previous paper by Pascual-Marqui reported that "The methodological developments have placed LORETA at a level that compares favourably to the more classical functional imaging methods, such as PET and fMRI". (Pascual-Marqui, 2002)

The Loreta method also has weaknesses, of course. It provides probabilistic and non-exact solutions of the EEG inverse problem, with a relatively low space resolution, which in any case is highly dependent on the number of electrodes.

In fact, as mentioned before, Loreta uses a standard brain template model. Methods such as fMRI and PET, on the contrary, provide their measures making use of an individual brain model, based on the specific subject's structural scan.

On the other hand, however, the improved version of Loreta provides 3D-images of standardized current density with zero-error localization property, and it is a non-

invasive and cheap method with an excellent temporal resolution, compared to the other functional imaging techniques.

But most importantly, Loreta is perfectly compatible with cochlear implant use. (Tang and Li, 2012)

## 2.3 Complexity of the EEG signal

Due to the stochastic nature of EEG signal, it might be interesting to evaluate its dynamic behavior. EEG signal complexity quantifies the brain dynamic, and a measure of EEG complexity may be carried out by means of the calculation of the Fractal Dimension. The Higuchi's algorithm is a good way to perform this measurement. (Vega and Nol, 2015)

The algorithm proposed by Higuchi for the calculation of the Fractal Dimension of a time series is based in the direct measure of the mean length of the curve L(k), by using a segment of k samples as measure unit. For different k values, a curve is said to have fractal dimension FD if

$$L(k) \sim k^{FD}$$

FD measures complexity of the curve and so of the time series that this curve represents, ranging from value 1 for deterministic flat curve to value 2 for a stochastic signal, as white noise.

## Aim of the Study

A synchronisation between auditory cortex and other cortical and subcortical centres is necessary for the properly functioning of the auditory system.

Hearing loss affects the normal development of connectivity between the auditory system and the higher neurocognitive functions.

Cochlear implant adds a new auditory modality in deaf patients, by bypassing the damaged elements of the ear and directly stimulating the auditory nerve. (Zeng, 2004)

The purpose of this study was to evaluate the effect of cochlear implantation on a group of deafness patient, in terms of restoration of auditory network.

In particular, the impact of age at time of first CI fitting and duration of CI use was analysed.

The difference between prelingual and postlingual deafness was also taken into account, in order to evaluate neural plasticity, both in the case of a limited access to the sounds from the very beginning, and in the case of a cortical network that has already been formed, before the onset of the hearing loss. (Dobie and Van Hemel, 2004)

Event Related Potentials and EEG patterns were analysed by applying a Low Resolution Tomography, in order to study the associative networks activated by the CI, cortical activation and functional connectivity.

# 3. Materials and Methods

The local institutional ethics committee approved the study. All experiments were conducted with the informed and overt consent of each participant.

## 3.1 Patients

Thirty patients with cochlear implant (mean age: 31.36 ± 18.10) were included in the study.

The inclusion criteria for the study group were:

- Prelingual or postlingual severe-to-profound bilateral sensorineural hearing loss
- use of CI
- no associated disabilities or diseases
- age over 10 years (younger children may have a very variable and unstable neuronal plasticity, and may have difficulties to correctly perform the required tasks)

Twenty-four were prelingually deaf patients. They were divided into two groups, according to the age at time of CI surgery: the early-implanted group included those implanted early in life, before 3 years old, while the late implanted group those fitted with cochlear implant at an older age, on average after fifteen years old.

Similarly, duration of CI use was dichotomized as short period of use, less than one year, and long period of use, on average more than three years.

Combining these two parameters, three clinical groups were obtained:

- GROUP A: early implanted and lengthy CI use
- GROUP B: late implanted and lengthy CI use
- GROUP C: late implanted and short CI use

A group of six patients with a postlingual deafness was also considered:

- GROUP D.

They were patients with a type of hearing loss which occurs after they have learned listening and language skills.

Each patient group was compared with a normal hearing control group, matched for mean age and sample size.

As regards cochlear implants, belonging to three CI brands (Advanced Bionics, Cochlear and MedEl) fifteen patients received their implant in the right ear, twelve in the left ear, and three received a bilateral cochlear implantation.

Hearing loss had arisen from different etiologies: Connexin 26, Rubella, familial and unknown etiology.

Auditory benefits from cochlear implantation were tested in all patients by free field pure tone audiometry. Pure Tone Average (PTA), expressed in decibels of hearing level (dB HL) and corresponding to the average air-tonal threshold at the frequencies of 500, 1000 and 2000 Hz, was calculated for each patient group.

The mean PTA was 31.4 dB HL (25-41 dB HL) for A group, 33.2 dB HL (22-43 dB HL) for B group, 45.1 dB HL (31-61 dB HL) for C group, and 31.5 dB HL (25-40 dB HL) for D group.

Control subjects had a normal hearing threshold levels (thresholds lower than 30 dB at all frequencies).

The characteristics of clinical groups are summarised in the table below.

*Table 3.1 Characteristics of the four clinical groups (patients and controls). Ages (in years) are expressed as mean ± SD and range.*

| CLINICAL GROUP | | PATIENTS | | CONTROLS | | T test (p) |
|---|---|---|---|---|---|---|
| A | **N** | 10 | | 10 | | |
| | **Age** | 13.30±3.08 | [10.50 – 20.00] | 13.54±3.66 | [10.08 -19.40] | 0.87 |
| | **CI Age** | 1.98±0.68 | [1.01 – 3.02] | | | |
| | **CI use** | 11.33±3.20 | [7.48 – 17.55] | | | |
| | **CI side** | R=5; L=3; Bil=2 | | | | |
| B | **N** | 7 | | 7 | | |
| | **Age** | 32.84±16.53; | [14.41 – 58.69] | 33.47±14.87 | [15.48 – 58.39] | 0.94 |
| | **CI Age** | 29.05±17.85 | [8.65 – 57.36] | | | |
| | **CI use** | 3.79±1.60 | [1.33 – 5.76] | | | |
| | **CI side** | R=4; L=3 | | | | |
| C | **N** | 7 | | 7 | | |
| | **Age** | 45.33±14.58 | [17.92 – 62.41] | 39.63±13.68 | [17.69 – 59.42] | 0.46 |
| | **CI Age** | 44.85±14.69 | [17.21 – 61.87] | | | |
| | **CI use** | 0.48±0.32 | [0.19 – 1.08] | | | |
| | **CI side** | R=2; L=5 | | | | |
| D | **N** | 6 | | 6 | | |
| | **Age** | 43.43±14.08 | [17.39 – 55.30] | 41.21±13.56 | [19.40 – 58.40] | 0.78 |
| | **CI Age** | 37.58±15.72 | [16.00 - 53.33] | | | |
| | **CI use** | 5.85±7.85 | [1.37 – 21.31] | | | |
| | **CI side** | R=4; L=1; Bil=1 | | | | |

## 3.2 Electrophysiological analysis

All the subjects underwent an electrophysiological evaluation, consisting of ERPs and EEG measurement.

Recordings were obtained with nineteen electrodes (Fp1, F3, C3, P3, O1, F7, T3, T5, Fz, Cz, Pz, Fp2, F4, C4, P4, O2, F8, T4, T6) positioned according to the International 10–20 System, with a linked ears reference. Each scalp electrode impedance was lower than 5 Kohm.

### 3.2.1 Event-related potentials (ERPs)

Long latency Auditory Evoked Potentials were performed. In particular, auditory elicitation of the P300 event-related evoked potential was analysed.

The sampling frequency was 2048 Hertz. A time window of 700 ms, 70 ms pre-stimulus and 630 ms post-stimulus, and an amplitude window of ± 70 μV were considered. A notch filter was used to remove 50 Hz contamination.

The active oddball paradigm was applied, to elicit the P300 wave. It consisted of a sequence of target and standard auditory stimuli, in a ratio of one to seven (60 target), randomly presented to the subject. The stimuli were pure tones of different frequencies, 1000 Hz for the standard, and 2000 Hz for the target. Both types of stimuli were characterized by the same intensity level and duration: 90 dB (comfortable for all patients) and 100 ms. The interstimulus interval (ISI) was 1020-1100 ms.

Headphones were used to deliver the stimuli to the microphone of the patient's speech processor.

All subjects were asked to keep count of all and only the target stimuli administered.

A band-pass filter [0.3 – 40 Hz] was applied to ERPs signals recorded from each subject.

Three different types of ERP signal analysis were performed:

- latency analysis
- cortical sources estimation
- time course analysis

Latency analysis:

The purpose of the first analysis was to evaluate the morphological features of the N200 and P300 waves.

We focused on Cz channel for the analysis, as it is generally regarded as the channel which provides the best evoked response.

Cortical sources estimation:

In this analysis, cortical sources of N200 and P300 waves and their intensity of activation were estimated using LORETA Software. The difference in cortical estimated

activation between patients and controls was then evaluated for each of the four clinical groups.

The pure target stimuli effect was considered for the estimation of cortical activity. It was delivered subtracting the standard stimulus response from the target one, for all the nineteen electrodes, and for each subject. This new function, the "pure target stimuli effect", was collapsed into 63 bins, each resulting from the averaged values of 10 ms. LORETA was then applied to this new function considering two time s: from 180 to 270 ms, and from 270 to 460 ms, the common of N200 and P300 elicitation for all groups, respectively.

Time course analysis

ERPs cortical source analysis provided a static representation of cortical activity, by calculating an estimate of the amount of activation in the different Brodmann areas, expressed as an average value on a defined time interval.

A time course analysis may be a complementary method to evaluate brain activation.

In this case, patterns of brain activity were analysed in terms of time courses of cortical activation.

For this purpose, the amount of activation was calculated as the sum of the activation values of all voxels belonging to a given BA, and it was analysed over the time interval from 180 to 460 ms (N200 and P300 elicitation), taking into account the areas found differently activated between patients and controls by the previous analysis.

### 3.2.2 Electroencephalographic recordings (EEG)

In the following step of the study, analysis of EEG epochs was carried out.

EEG recordings were obtained using a sampling rate of 128 Hz.

The recordings were performed under two different conditions: resting state, during which the subjects were asked to stay relaxed, without explicit tasks to be done, and activation state, during which the subjects were asked to remember two short stories, narrated without prosody, that they had been listened before. Each subject was also asked to repeat the stories as precisely as possible, in order to verify that they had been effectively listened and memorized.

The two stories used in this analysis are designed to provide information on immediate verbal memory, and they are included in a battery of neuropsychological tests. (Mondini, 2003)

About four minutes of resting state and four minutes of activation state EEG data were collected for each subject. In both cases, EEG activity was recorded during eyes-closed condition.

Thereafter, these data were elaborated with the use of the software EAGLE, in order to visually choose artefact free epochs from the continuous EEG signal.

EAGLE is a self-written matlab software that allows a user to view EEG patterns and extract EEG data epochs in text format, available for use by LORETA software.

The band-pass filter [2 – 40 Hz] was then applied. A variable number of EEG epochs, 20 – 30, each of 4 seconds duration, were collected for each recording.

They were then processed using LORETA software.

EEG evaluation consist of:

- study of functional connectivity
- study of complexity of signal

Functional connectivity

In this analysis, functional brain connectivity was analysed in frequency domain, in all four clinical groups.

The lagged coherence was calculated between Brodmann areas belonging to Default Mode Network, left and right Precuneus and associative visual cortex, for each of the five frequency bands (delta, theta, alpha1, alpha2 and beta), and for each of the two conditions (resting state and activation state).

Default Mode Network (DMN) is a complex brain network of interacting cortical and subcortical regions, more involved at rest than during a specific task performance. (Uddin et al, 2009)

fMRI studies during tasks compared to rest have shown that DMN tends to reduced its activity during a specific task. In other words, DMN is generally considered to be active when a subject is not involved in performing specific tasks and his brain is at wakeful rest. (Raichle et al, 2001; Blumenfeld, 2016)

However, as it is known today, DMN may also correlate with other networks and it may be positively activated in relation to any external task performance, such as working memory tasks. (Spreng, 2012)

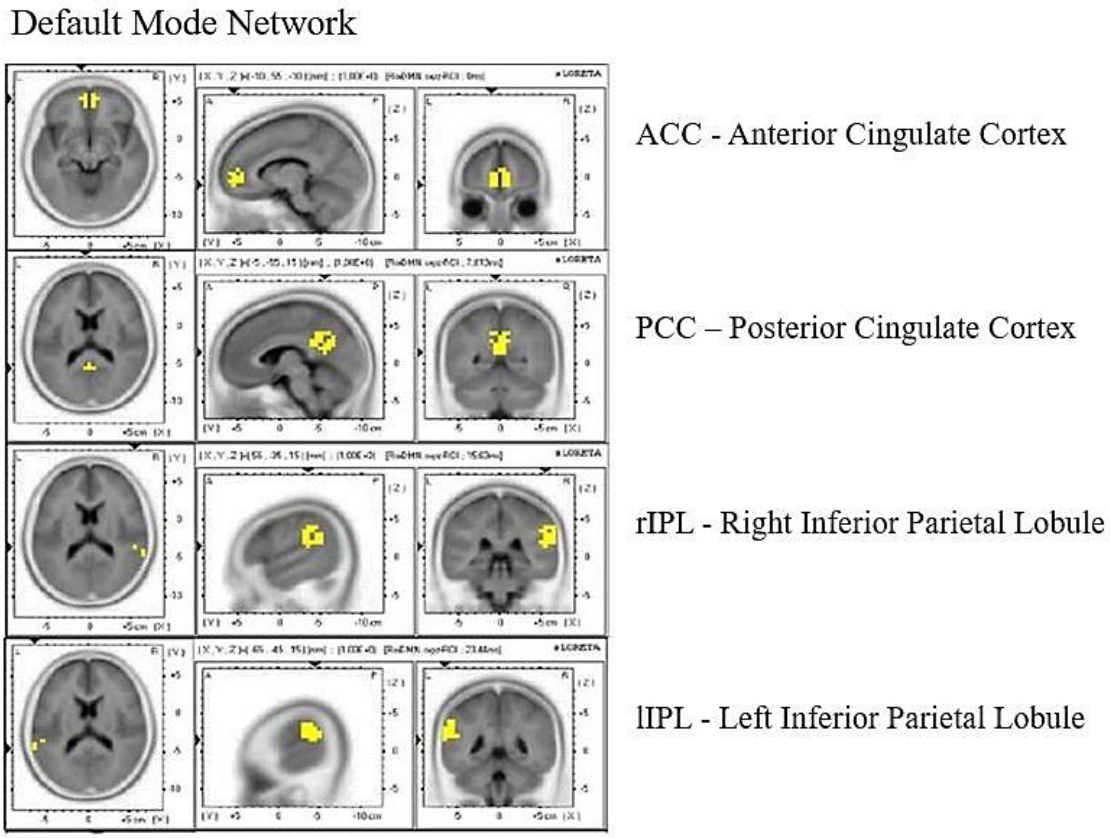


*Figure 3.2.2.1. Regions of interest (ROIs) in the default mode network (DMN)*

The precuneus is a brain region which is part of the superior parietal lobule, located in front of the occipital lobe. It is characterized by one of the highest resting metabolic rates, showing an activity decrease during nonself-referential goal-directed tasks.
Generally, however, the connectivity of the precuneus is made of several connections with the higher association cortical and subcortical structures. Brain connectivity studies have shown how the precuneus is actually involved in a lot of cognitive processes, including memory tasks. Considering that no direct connections between precuneus and the primary sensory cortex have been found, it is believed that precuneus activity does not have a direct impact on stimulus processing, but instead is able to influence cortical and subcortical networks involved in elaborating highly integrated information. (Cavanna and Trimble, 2006)

Precuneus

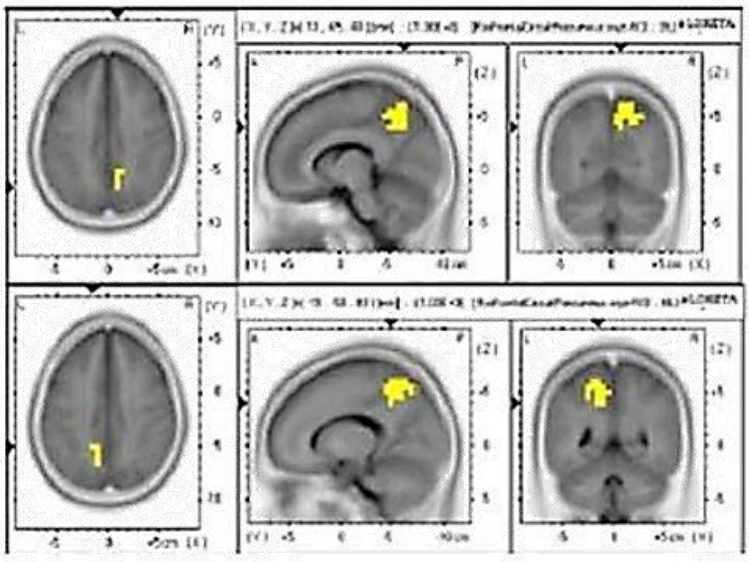

rPC - Right Precuneus

lPC – Left Precuneus

*Figure 3.2.2.2. Regions of interest (ROIs) in the Precuneus*

The visual cortex is a brain area located in the occipital lobe, involved in visual information processing.

It is known that in case of sensory deprivation there is an adaptive and compensatory mechanism, involving a functional recruitment of brain regions usually related with the deprived sensory modality by those sensory modalities that are not compromised. (Merabet and Pascual-Leone, 2010)

In case of hearing loss, auditory cortical areas do not receive normal sensory input, and brain areas normally involved in sound processing may be reorganized by other sensory modalities, such as the visual one, through a mechanism called cross-modal neuroplasticity. (Sharma and Glick, 2018)

Complexity of signal

The possibility that there was a difference in terms of complexity of EEG signal between patients and controls, and between resting and activation state, was taken into account. For this purpose, a measurement of EEG complexity was performed by calculation of Fractal Dimension, by applying the Higuchi's algorithm.

In this analysis, EEG complexity was calculated for the whole patient group and for the whole control group.

## 3.3 Statistical analysis

All statistical analyses were performed using the Statistica 12.0 software package and LORETA software. The significance level was set at $p < 0.05$.

Normality of data was checked using the Kolmogorov Smirnov test.

The t-test for independent groups was used for comparing latencies in the group as a whole (patients versus controls), and in all clinical groups.

As regards the cortical sources analysis, LORETA Student's t-test was used on log-normalized data. Correction for multiple comparisons was performed using the randomization approach with 5000 randomizations.

A LORETA monovariate regression analysis with duration of CI use and age of CI surgery as covariates was also performed in the prelingual group, to evaluate the relation between cortical activation and the two implantation covariates taken into account.

# 4. Results

## 4.1 ERPs analysis

First thing, it should be said that all subjects, both the patients and the controls, correctly identified all the target stimuli during auditory oddball task.

### 4.1.1 Latency analysis

The following results were obtained from the analysis of the ERPs latencies:

*Table 4.1.1.1. Mean latency values of N100, N200 and P300 potentials in patients and control subjects*

| | | **N100** | **p** | **N200** | **p** | **P300** | **p** |
|---|---|---|---|---|---|---|---|
| **TOTAL Group** | Patients | 123±20 | <0.001 | 229±33 | 0.006 | 350±42 | <0.001 |
| | Controls | 98±16 | | 210±14 | | 309±16 | |
| **A Group** | Patients | 118±18 | 0.44 | 234±38 | 0.20 | 352±45 | 0.01 |
| | Controls | 111±21 | | 217±14 | | 307±16 | |
| **B Group** | Patients | 128±22 | 0.01 | 221±34 | 0.30 | 340±30 | 0.01 |
| | Controls | 90±7 | | 206±15 | | 303±16 | |
| **C Group** | Patients | 139±17 | <0.001 | 248±28 | 0.004 | 378±51 | 0.006 |
| | Controls | 93±6 | | 205±15 | | 311±17 | |
| **D Group** | Patients | 109±14 | 0.04 | 209±12 | 0.7 | 328±21 | 0.3 |
| | Controls | 94±7 | | 211±10 | | 318±16 | |

Comparing patients and controls in the study population as a whole, the N100, N200 and P300 latencies were significantly longer in patients than in controls.

However, looking at the individual clinical groups, results showed significant difference between patients and control included in the A group only as regards the P300 latency. The D group differ significantly in only N100 latency. A significant difference between patients and controls was found in the B group, both in N100 and in P300, while all latencies of the C group were found to be significantly longer in patients than the respective controls.

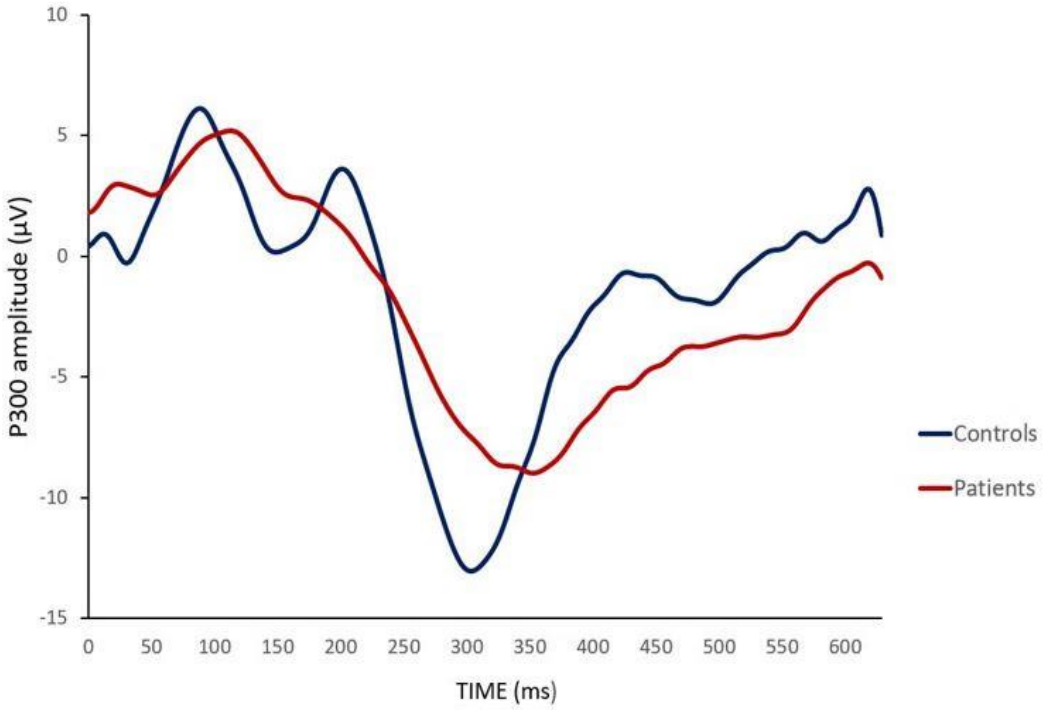


*Figure 4.1.1.1. Grand average of target stimuli recorded in Cz. Data were considered, respectively, in the whole patient and control group.*

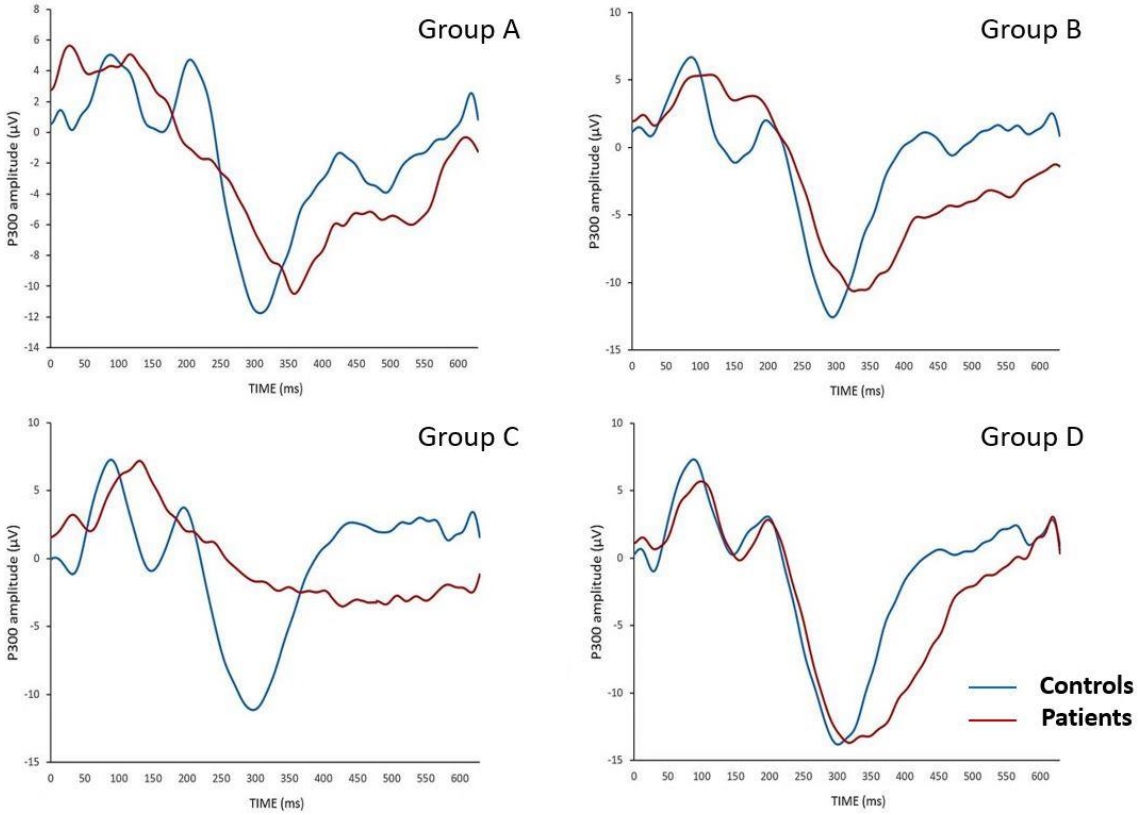


*Figure 4.1.1.2. Grand average of target stimuli recorded in Cz, for each of the four groups.*

Grand average event related potentials of the controls are almost identical in all the four groups. However, with regard to patient latencies, they are similar to those of normal hearing controls in A, B and D groups, while patients belonging to the C group showed ERPs components characterized by a very low amplitude and a large P3 component. Furthermore, only N100 peak was clearly detectable in this group.

### 4.1.2 Cortical source analysis

Cortical difference of activation between patients and controls are presented through LORETA probabilistic maps for each of the four groups.

Warm coloured areas represent a greater activation in control group, more evident from dark red to yellow. On the contrary, cold coloured areas represent a greater activation in patient group, more evident from dark to light.

When considering prelingual patients, no difference in cortical activation between patients and controls was found in the A group, neither with regard to N200 elicitation (time window from 180 to 270 ms) nor for P300 (time window from 270 to 460ms).

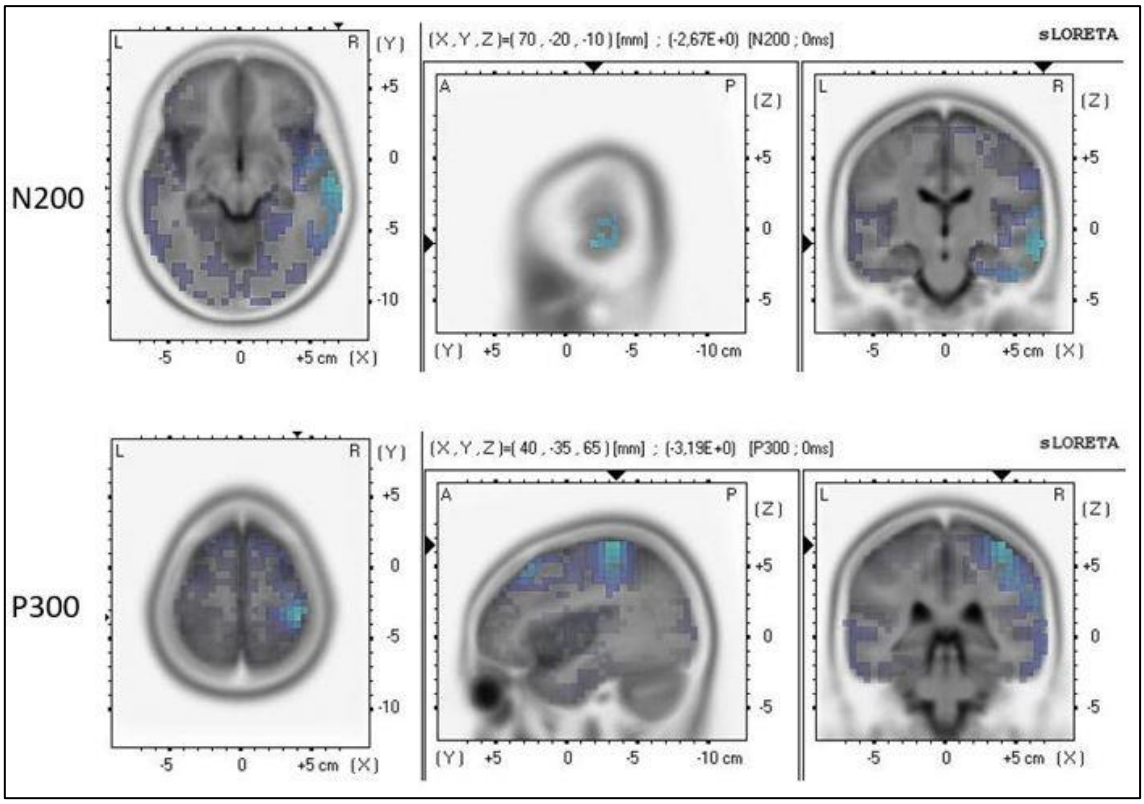


*Figure 4.1.2.1. LORETA probabilistic maps of the cortical activation - group A. No significant difference was found neither in N200 (above) nor in P300 (below).*

Group B showed a greater activation in frontal areas both as regard N200 and P300 wave in controls compared with patients, but the difference was not statistically significant.

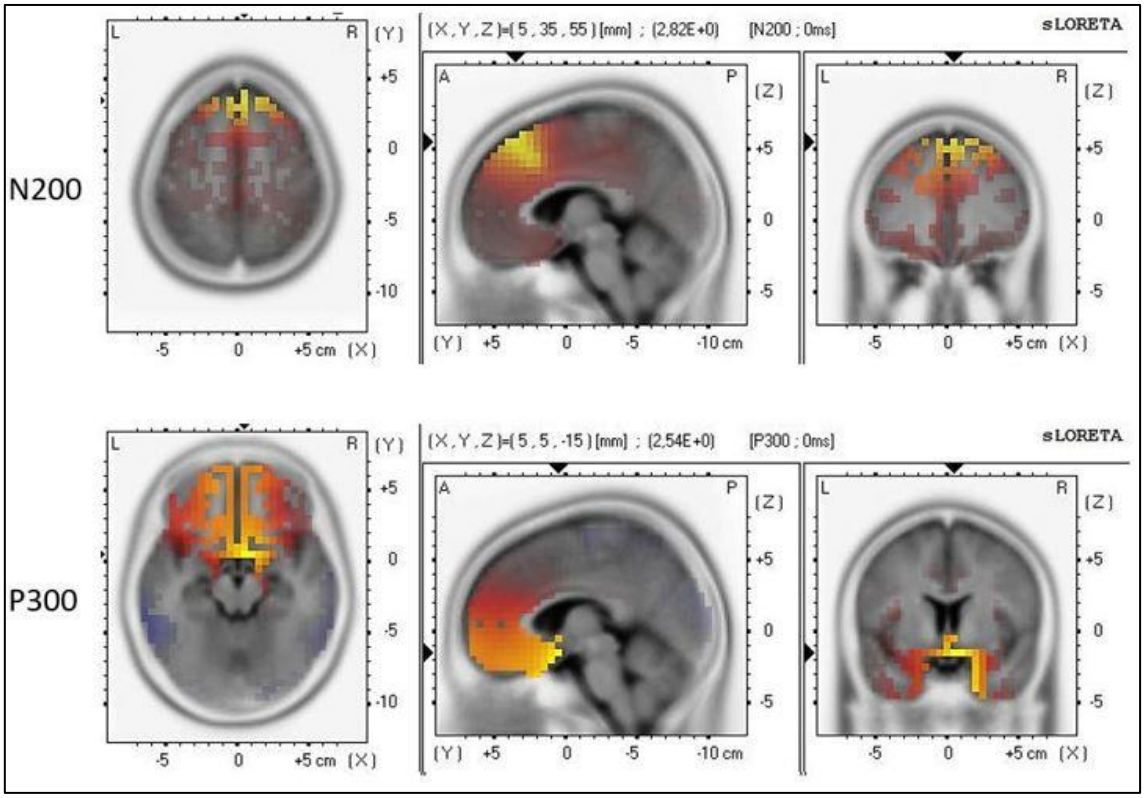


*Figure 4.1.2.2. LORETA probabilistic maps of the cortical activation - group B. A greater activation was found in controls, but this difference was not statistically significant neither in N200 (above) nor in P300 (below).*

The difference between patients and controls belonging to the C group, on the other hand, reached statistical significance ($p<0.01$). More specifically, in the N200 time window, controls showed a higher cortical activation in frontal areas (Brodmann areas 8, 9 and 10) and in the cingulate cortex (Brodmann areas 24, 32 and 33), and in the P300 time window a significantly higher activation of control group was found again in frontal areas (Brodmann areas 10, 11, and 25) and in cingulate cortex (BA 32).

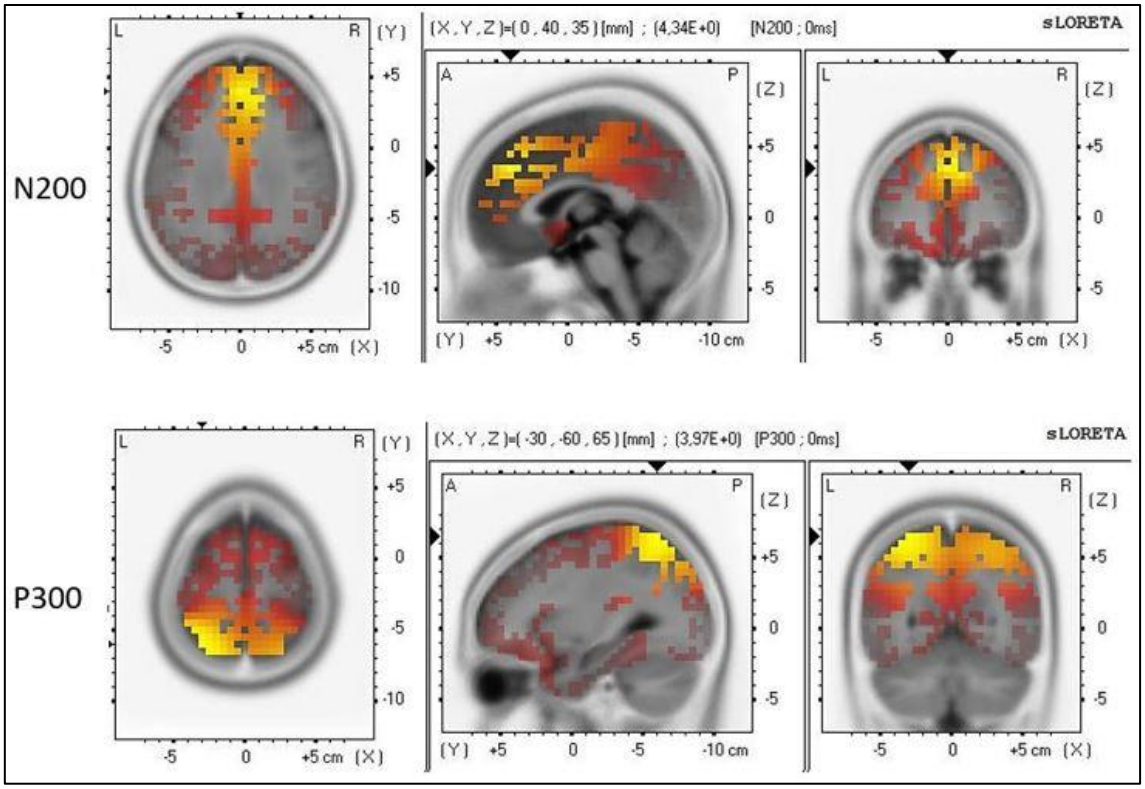


*Figure 4.1.2.3. LORETA probabilistic maps of the cortical activation - group C. A greater activation in control group was found in the frontal areas and cingulate cortex: this difference was statistically significant both in N200 (above) and in P300 (below).*

A comparable activation between postlingual patients and their relative controls was found in the D group.

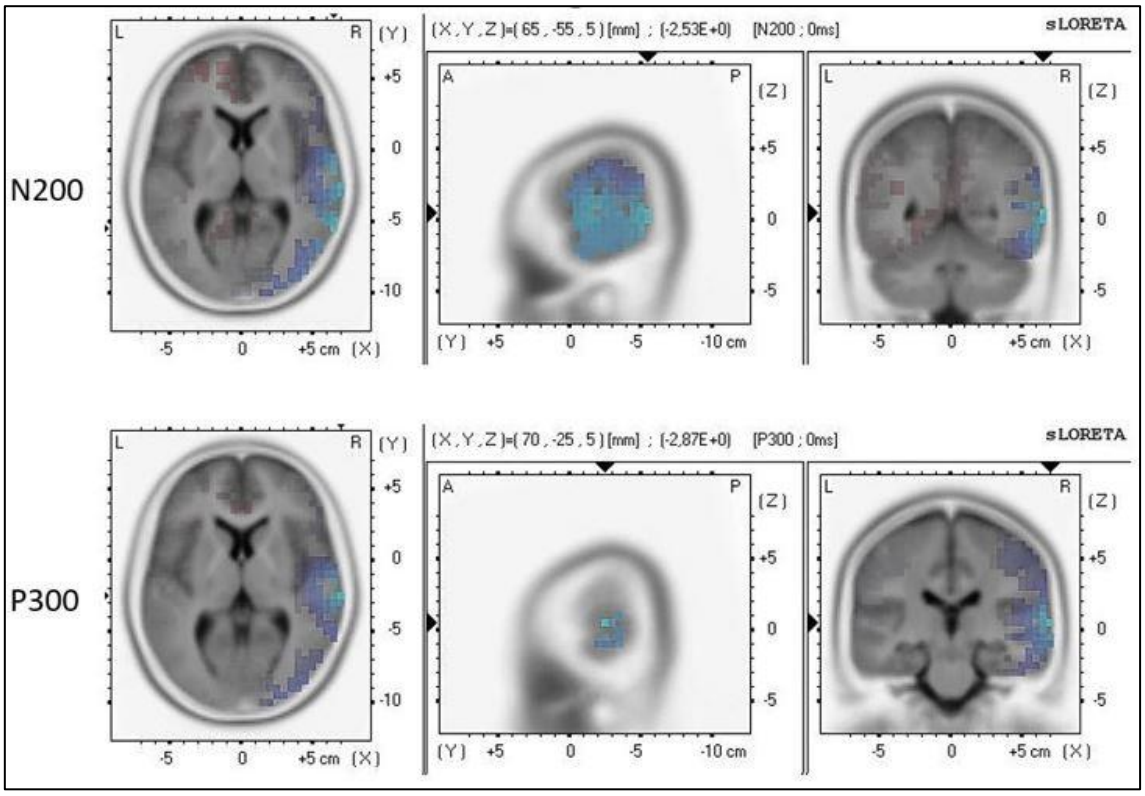


*Figure 4.1.2.4. LORETA probabilistic maps of the cortical activation - group D. No significant difference in activation was found neither in N200 (above) nor in P300 (below).*

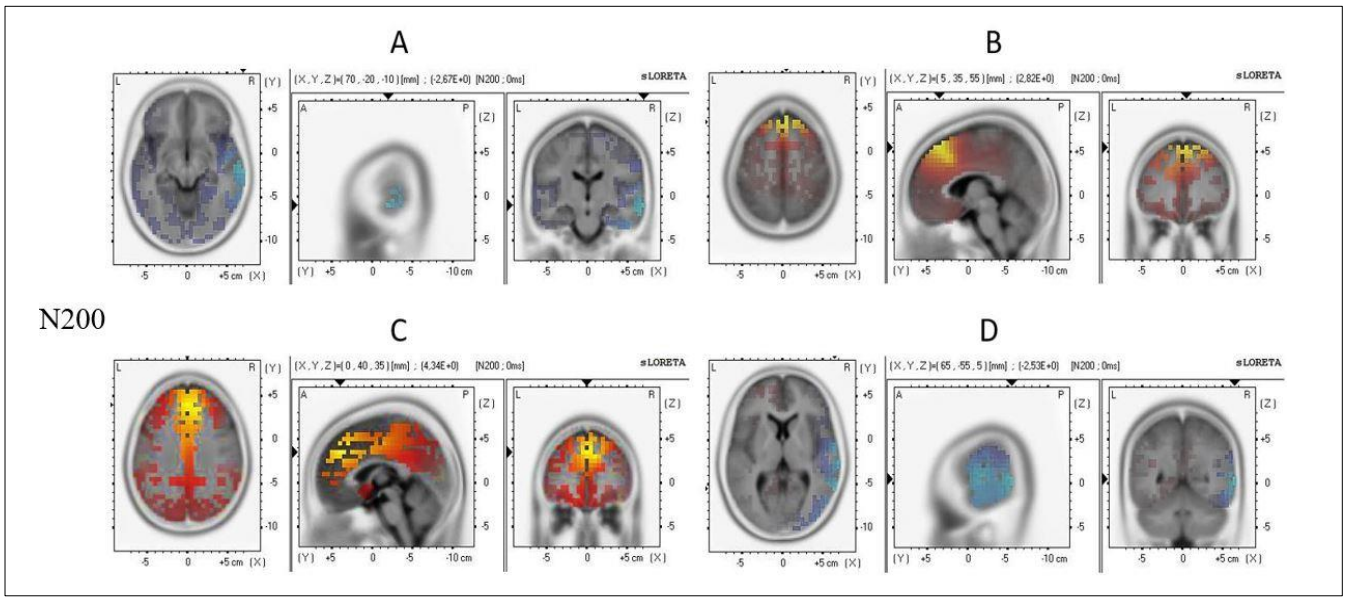


*Figure 4.1.2.5. Summary of probabilistic Loreta maps of the four groups - N200 elicitation.*

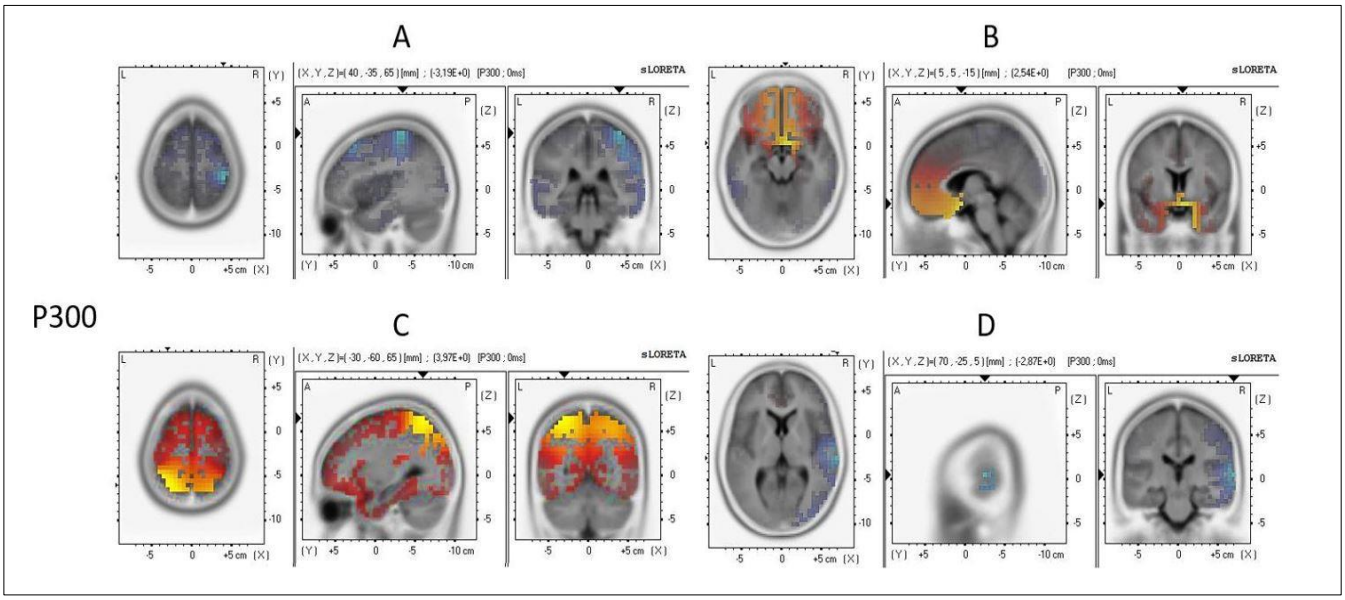


*Figure 4.1.2.6. Summary of probabilistic Loreta maps of the four groups – P300 elicitation.*

Linear regression analysis showed that the amount of cortical activation is significantly directly correlated with duration of implant use and significantly inversely correlated with age at implant, for both N200 and P300 potentials.

*Table 4.1.2.1. Linear correlation coefficient (r) and corresponding significance between amount of cortical activation and respectively age of CI surgery and duration of CI use.*

| | Correlation Coefficient (R) | | P |
|---|---|---|---|
| | N200 | P300 | |
| **Age of CI surgery** | R = -0.74 | R = -0.76 | P < 0.01 |
| **Duration of CI use** | R = 0.70 | R = 0.77 | P < 0.01 |

## 4.1.3 Time course analysis

The time course of activation is a representation of the electrical strength over the time interval during which N200 and P300 are elicitated (time window from 180 to 460 ms).
The cortical activation values of Brodmann areas 8, 9, 10, 11 and 25 were aggregated to obtain a single frontal area. The same applied for Brodmann areas 24, 32 and 33, to obtain a single cingulate area.
This allowed to simplify the comparison between patients and controls, in all the four groups.
In all control groups both the frontal and the cingulate areas showed a regular and cyclic pattern, with maxima related to the N200 and P300 wave apex.
When controls were compared with patients in the four clinical groups, a comparable activation in strength and timing between patients and controls was only found in the A prelingual patient group and D postlingual group.
This consideration may also be extended to the second prelingual group, the B group, even if to a lesser extent.
Conversely, there was a marked difference in the third prelingual clinical group (C), whose patients showed a very low cortical activation, with no cyclic pattern.

It is worth noting that, while all four control groups very clearly showed a peak relating to N200 and a pronounced concavity for both the frontal and the cingulate areas, these features were totally lacking in all four patient groups.

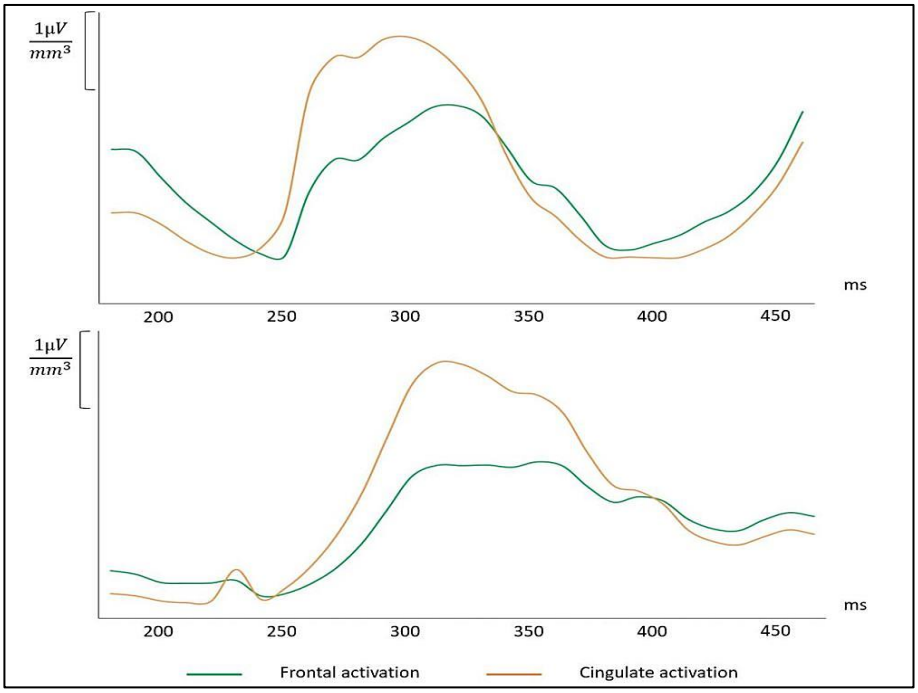


*Figure 4.1.3.1. Time course analysis of frontal and cingulate activation from 180 to 460 ms in controls (above) and patients (below) – Group A*

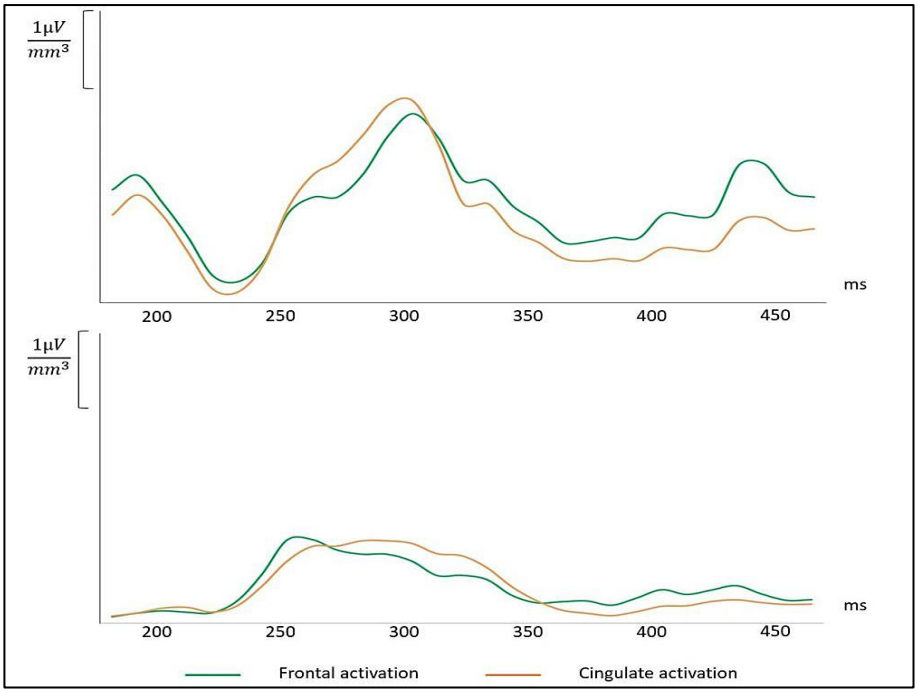


*Figure 4.1.3.2. Time course analysis of frontal and cingulate activation from 180 to 460 ms in controls (above) and patients (below) – Group B*

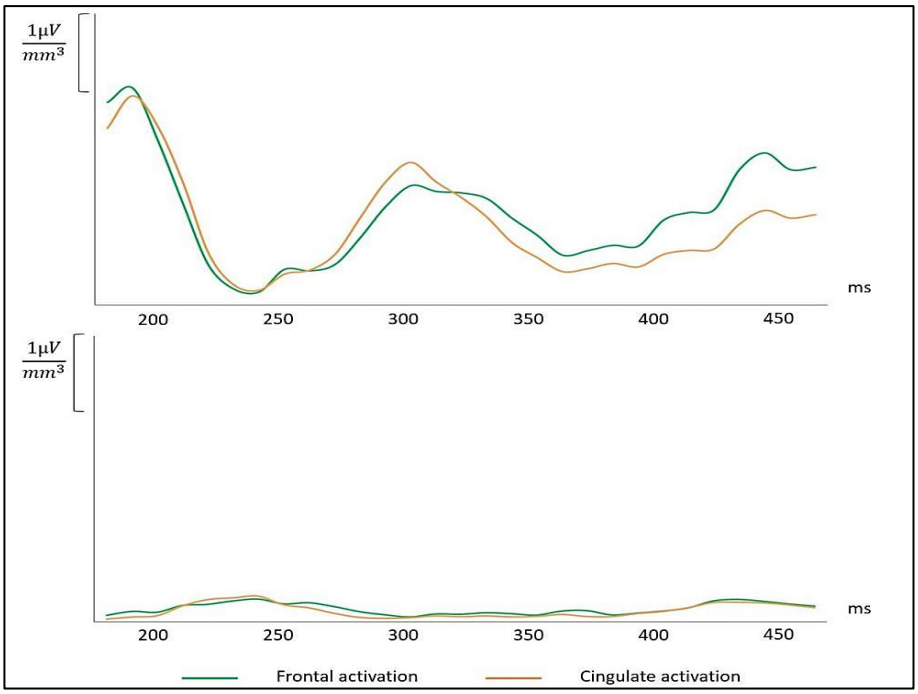


*Figure 4.1.3.3. Time course analysis of frontal and cingulate activation from 180 to 460 ms in controls (above) and patients (below) – Group C*

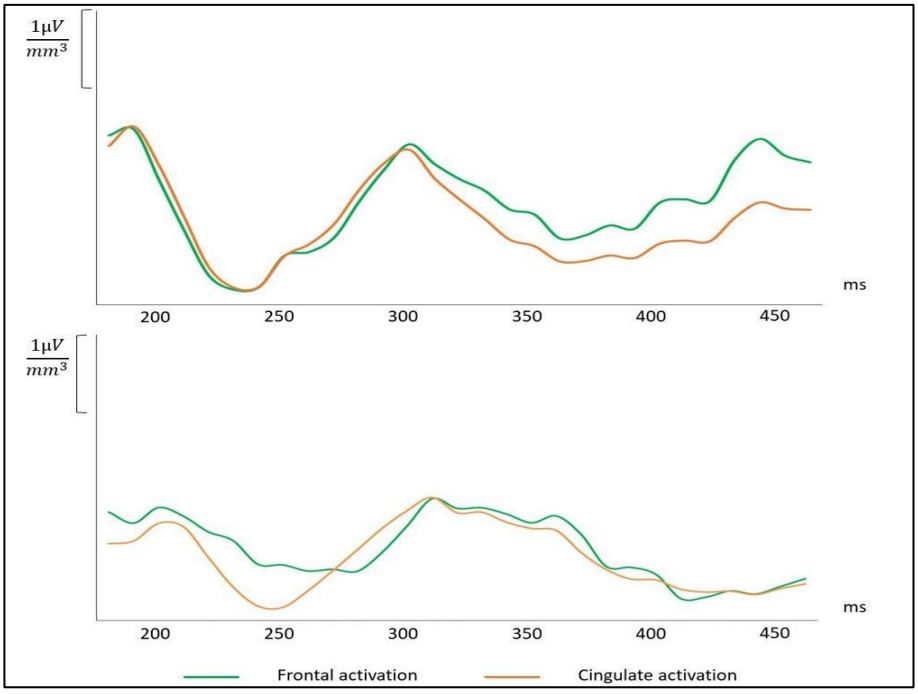


*Figure 4.1.3.4. Time course analysis of frontal and cingulate activation from 180 to 460 ms in controls (above) and patients (below) – Group D*

## 4.2 EEG analysis

### 4.2.1 Functional Connectivity

Coherence was calculated at each of five frequency bands (delta, theta, alpha1, alpha2 and beta), separately for each of the four distinct groups, and by evaluating the effect of the two different conditions (resting state and activation state).

The most relevant coherence differences between patients and controls were found in the alpha band, especially for the activation state.

Functional connectivity results are presented in the form of line graphs showing the coherence values in the alpha1 band. On the x axis 136 pairs of ROIs are represented, as 17 regions of interest were selected for the connectivity analysis: Anterior cingulate cortex – dorsal (ACC), Anterior cingulate cortex – ventral (ACC), Right superior frontal gyrus (rSFG), Left superior frontal gyrus (lSFG), Right middle frontal gyrus (rMFG), Left middle frontal gyrus (lMFG), Posterior cingulate cortex (PCC), Right inferior parietal lobule (rIPL), Left inferior parietal lobule (lIPL), Right precuneus (rPC), Left precuneus (lPC), Right temporal (rTemp), Left temporal (lTemp), Brodmann area 18 (BA18), Brodmann area 19 (BA19).

*Table 4.2.1.1. Pairs of ROIs included in the connectivity analysis*

| | | | | | | | | | | | |
|---|---|---|---|---|---|---|---|---|---|---|---|
| 1 | ACC-rSFG | 24 | lSFG-rMFG | 47 | lMFG-rPC | 70 | lIPL-lPC | 93 | rMFG-BA19DX | 116 | rPC-BA18SIN |
| 2 | ACC-lSFG | 25 | lSFG-lMFG | 48 | lMFG-lPC | 71 | lIPL-rTemp | 94 | rMFG-BA19SIN | 117 | rPC-BA19DX |
| 3 | ACC-rMFG | 26 | lSFG-ACC | 49 | lMFG-rTemp | 72 | lIPL-lTemp | 95 | lMFG-BA18DX | 118 | rPC-BA19SIN |
| 4 | ACC-lMFG | 27 | lSFG-PCC | 50 | lMFG-lTemp | 73 | rPC-lPC | 96 | lMFG-BA18SIN | 119 | lPC-BA18DX |
| 5 | ACC-ACC | 28 | lSFG-rIPL | 51 | ACC-PCC | 74 | rPC-rTemp | 97 | lMFG-BA19DX | 120 | lPC-BA18SIN |
| 6 | ACC-PCC | 29 | lSFG-lIPL | 52 | ACC-rIPL | 75 | rPC-lTemp | 98 | lMFG-BA19SIN | 121 | lPC-BA19DX |
| 7 | ACC-rIPL | 30 | lSFG-rPC | 53 | ACC-lIPL | 76 | lPC-rTemp | 99 | ACC-BA18DX | 122 | lPC-BA19SIN |
| 8 | ACC-lIPL | 31 | lSFG-lPC | 54 | ACC-rPC | 77 | lPC-lTemp | 100 | ACC-BA18SIN | 123 | rTemp-BA18DX |
| 9 | ACC-rPC | 32 | lSFG-rTemp | 55 | ACC-lPC | 78 | rTemp-lTemp | 101 | ACC-BA19DX | 124 | rTemp-BA18SIN |
| 10 | ACC-lPC | 33 | lSFG-lTemp | 56 | ACC-rTemp | 79 | ACC-BA18DX | 102 | ACC-BA19SIN | 125 | rTemp-BA19DX |
| 11 | ACC-rTemp | 34 | rMFG-lMFG | 57 | ACC-lTemp | 80 | ACC-BA18SIN | 103 | PCC-BA18DX | 126 | rTemp-BA19SIN |
| 12 | ACC-lTemp | 35 | rMFG-ACC | 58 | PCC-rIPL | 81 | ACC-BA19DX | 104 | PCC-BA18SIN | 127 | lTemp-BA18DX |
| 13 | rSFG-lSFG | 36 | rMFG-PCC | 59 | PCC-lIPL | 82 | ACC-BA19SIN | 105 | PCC-BA19DX | 128 | lTemp-BA18SIN |
| 14 | rSFG-rMFG | 37 | rMFG-rIPL | 60 | PCC-rPC | 83 | rSFG-BA18DX | 106 | PCC-BA19SIN | 129 | lTemp-BA19DX |
| 15 | rSFG-lMFG | 38 | rMFG-lIPL | 61 | PCC-lPC | 84 | rSFG-BA18SIN | 107 | rIPL-BA18DX | 130 | lTemp-BA19SIN |
| 16 | rSFG-ACC | 39 | rMFG-rPC | 62 | PCC-rTemp | 85 | rSFG-BA19DX | 108 | rIPL-BA18SIN | 131 | BA18DX-BA18SIN |
| 17 | rSFG-PCC | 40 | rMFG-lPC | 63 | PCC-lTemp | 86 | rSFG-BA19SIN | 109 | rIPL-BA19DX | 132 | BA18DX-BA19DX |
| 18 | rSFG-rIPL | 41 | rMFG-rTemp | 64 | rIPL-lIPL | 87 | lSFG-BA18DX | 110 | rIPL-BA19SIN | 133 | BA18DX-BA19SIN |
| 19 | rSFG-lIPL | 42 | rMFG-lTemp | 65 | rIPL-rPC | 88 | lSFG-BA18SIN | 111 | lIPL-BA18DX | 134 | BA18SIN-BA19DX |
| 20 | rSFG-rPC | 43 | lMFG-ACC | 66 | rIPL-lPC | 89 | lSFG-BA19DX | 112 | lIPL-BA18SIN | 135 | BA18SIN-BA19SIN |
| 21 | rSFG-lPC | 44 | lMFG-PCC | 67 | rIPL-rTemp | 90 | lSFG-BA19SIN | 113 | lIPL-BA19DX | 136 | BA19DX-BA19SIN |
| 22 | rSFG-rTemp | 45 | lMFG-rIPL | 68 | rIPL-lTemp | 91 | rMFG-BA18DX | 114 | lIPL-BA19SIN | | |
| 23 | rSFG-lTemp | 46 | lMFG-lIPL | 69 | lIPL-rPC | 92 | rMFG-BA18SIN | 115 | rPC-BA18DX | | |

No difference in coherence values between patients and controls was found in the A group.

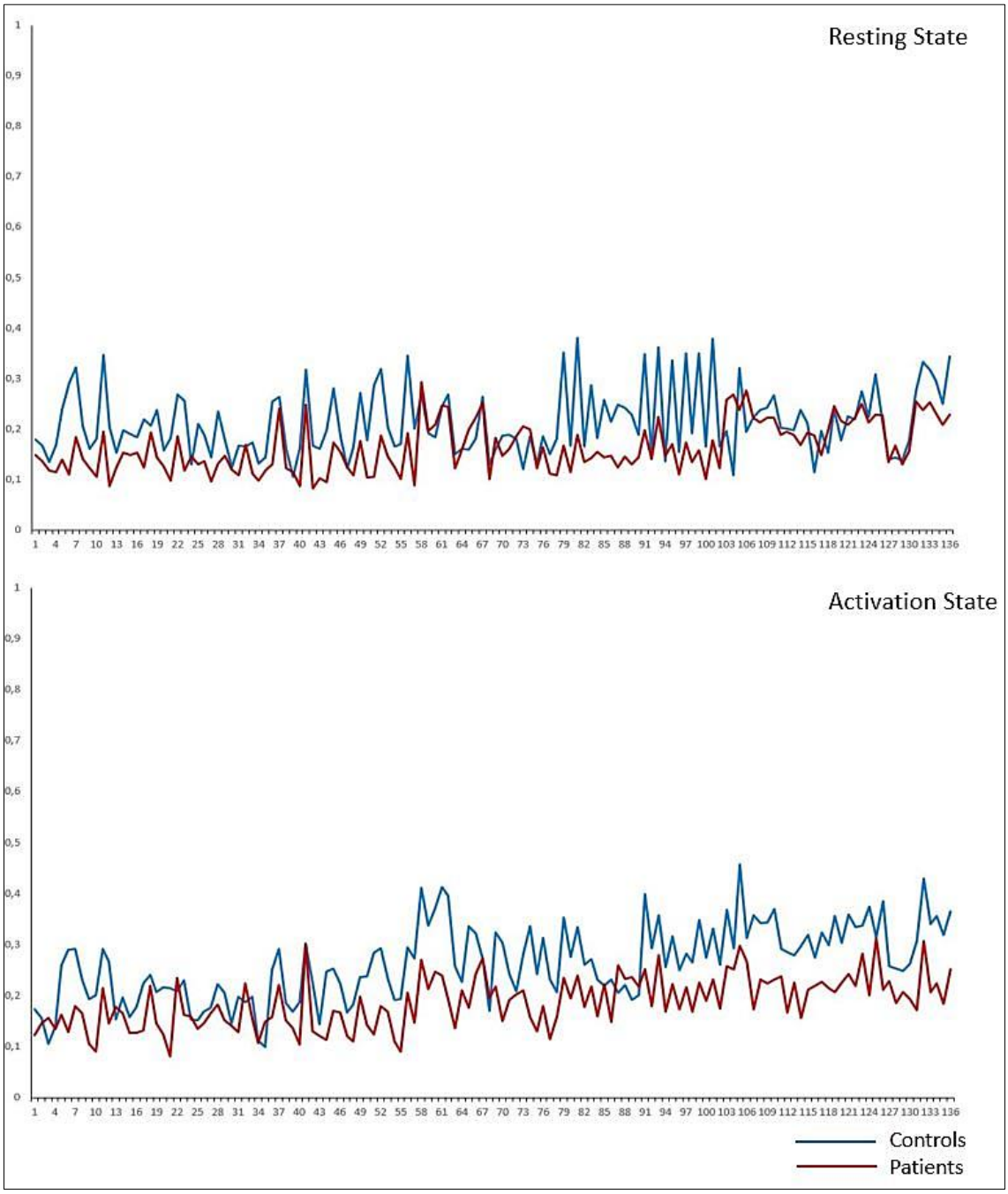


*Figure 4.2.1.1. Functional connectivity between ROI pairs – Group A*

Functional connectivity showed a significant increase in the B and C patient group, especially in the activation state, and specifically between visual areas and Precuneus and posterior cingulate cortex.

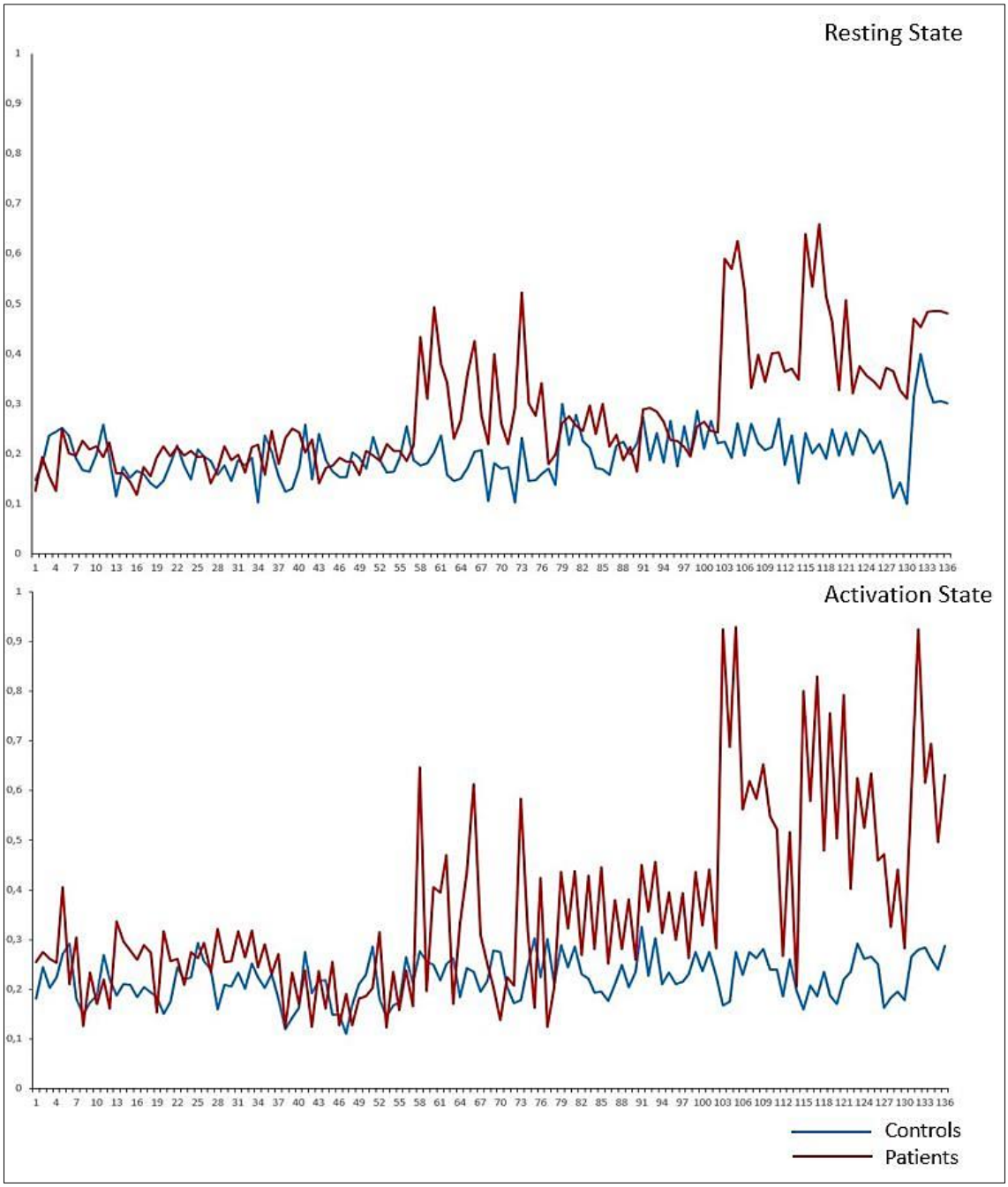


*Figure 1.2.1.2. Functional connectivity between ROI pairs – Group B*

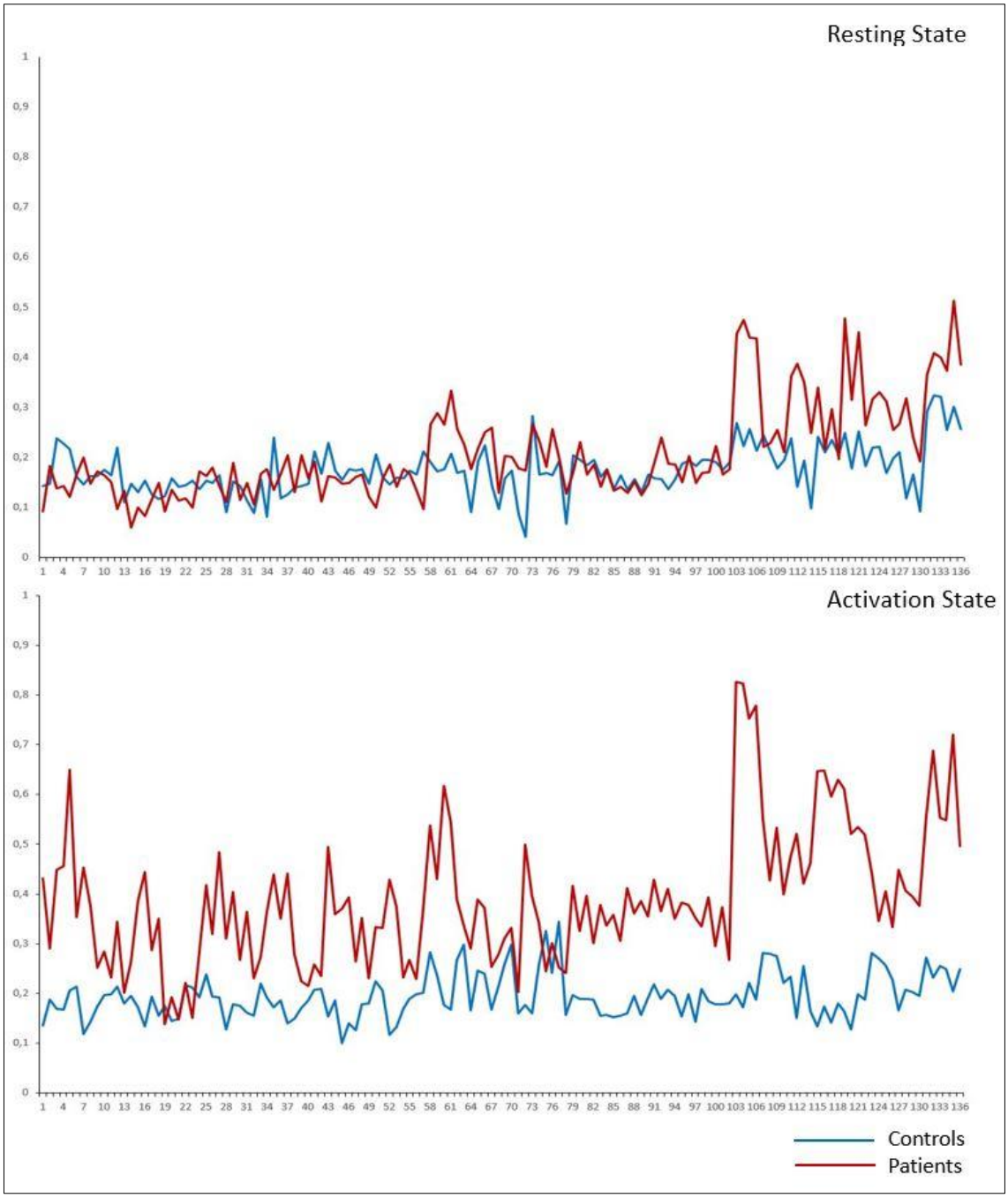


*Figure 4.2.1.3. Functional connectivity between ROI pairs – Group C*

Even in this analysis, postlingual patients showed no difference compared to controls.

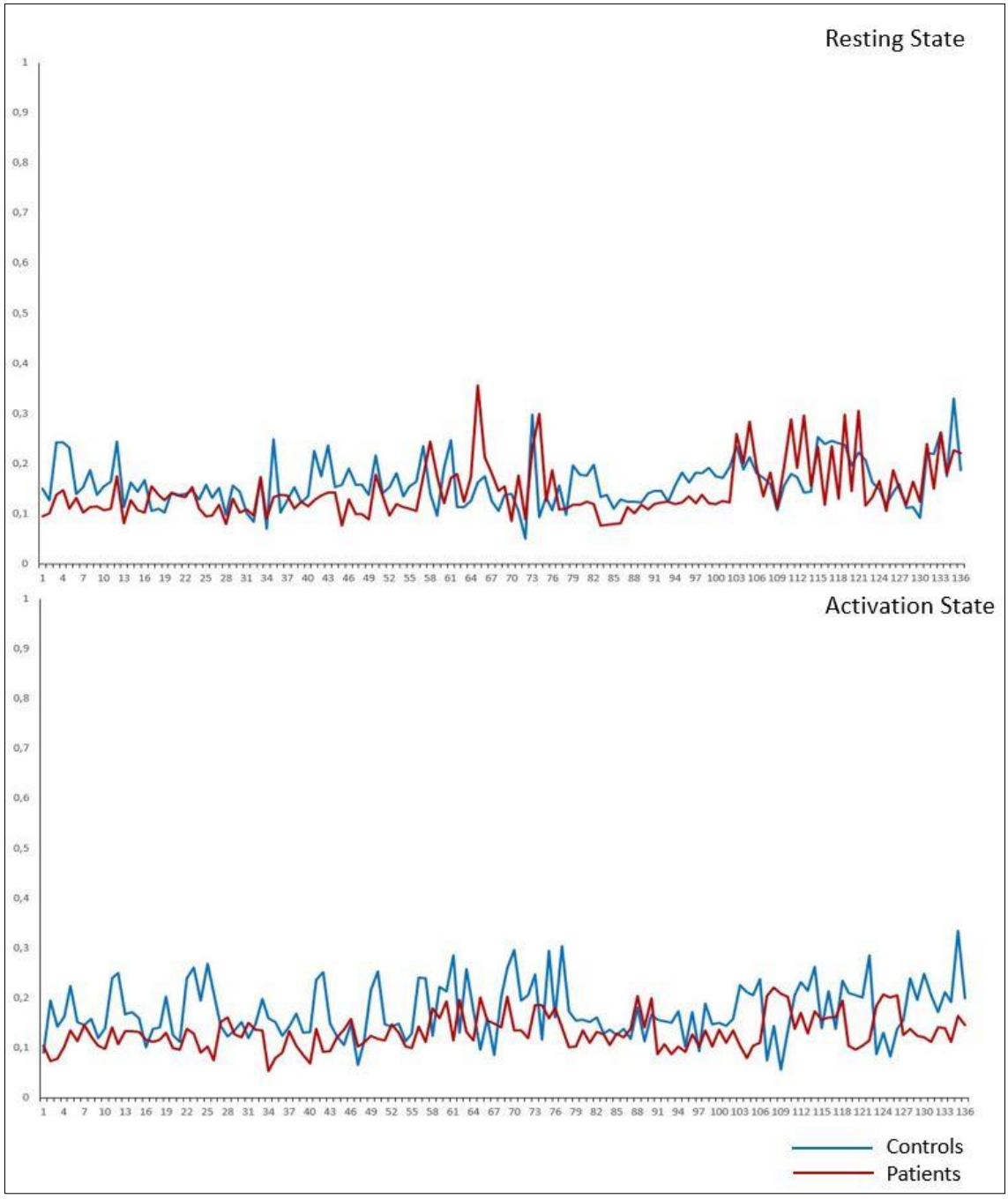


*Figure 4.2.1.4. Functional connectivity between ROI pairs – Group D*

### 4.2.2 Complexity of signal

The values of the complexity measures from EEG signals are shown in the figure below, for each of the EEG channels.

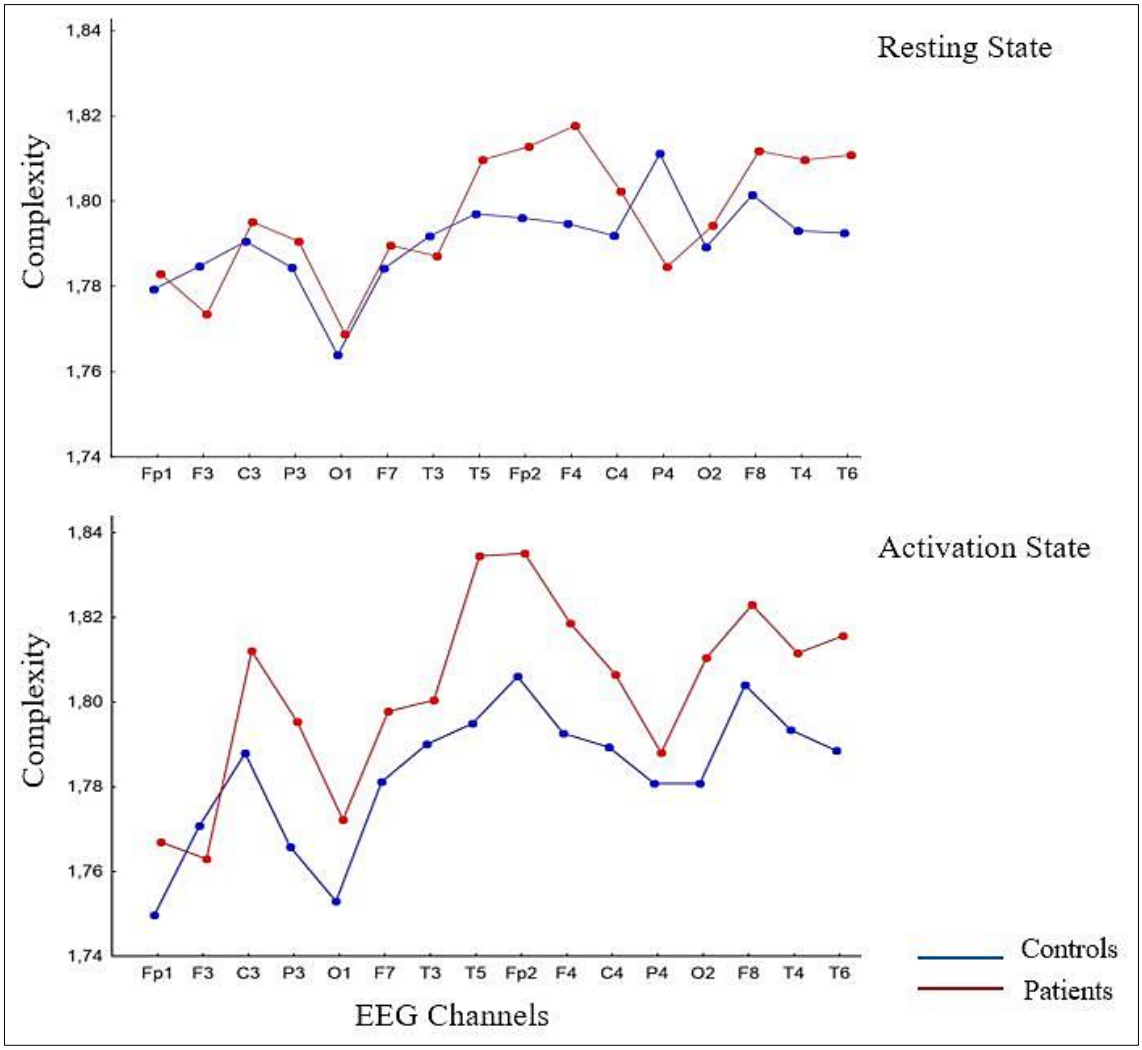


*Figure 4.2.2.1 Complexity of EEG signal calculated using Higuchi algorithm.*

It can be seen that patients showed higher complexity values than controls (not significantly relevant), and that particularly when examining the activation state.

This is, however, a result which does not allow a reasonable interpretation, but which may be a starting point for any future evaluations.

# 5. Discussion

In this study, as stated above, the associative networks activated by acoustic stimulation were investigated in deaf patients with Cochlear Implant.
By comparing them with normal-hearing controls, the following questions were assessed:

- the impact of the interaction between age at time of first CI fitting and duration of CI use in the restoration of auditory perception
- the degree of impairment due to the prelingual or postlingual acoustic deprivation

The latency analysis showed a significant increase in the N100, N200 and P300 peaks when comparing the whole group of patients with controls. This feature was only observed in in group C, while group A and B showed a significant difference only in P300 latency and in P300 and in N100 latencies respectively. In the D group the significance was reached for N100 latency. The results of C group are clear, while the differences observed in the other groups are probably due to a β error type. However, it is important to make it clear that three single measures (latencies of N100, N200 and P300) may be inappropriate in depicting a complex event like an evoked potential which is a complex time series.

LORETA cortical analysis showed a very clear difference when comparing the third group of patients (group C) with an age-matched control group. This clinical group consist of patients with long-term auditory deprivation who had been using CI for only a very short time (less than one year).
A statistically higher amount of cortical activation in the frontal areas and cingulate cortex was observed in the C control group compared to C patients, for both the N200 and the P300 waves.
On the contrary, a comparison between an early-implanted patient group with a long term CI use (group A) and their control group showed no differences, neither for N200 nor for P300 potential.
The advantages of early implantation in terms of audiological performances are very well known (Sharma et al, 2002), but it is interesting how early implantation, combined

with a long-term CI use, seems to be associated with a normalization process from a neurophysiological standpoint too.

As regards prelingual deafness, group A and Group C represent two extreme conditions: early implant and long CI use versus late implant and short time of CI use.

An intermediate condition is represented by patients in the B group (late implant, and long CI use).

In this case, the comparison between patients and an age-matched control group, showed a higher level of cortical activation in the control subjects, but this is a not statistically significant difference.

These findings are consistent with the LORETA monovariate regression analysis performed in prelingual patients: the amount of cortical activation was found to be significantly directly correlated with duration of implant use and significantly inversely correlated with age at implant for both N200 and P300 waves. (Unfortunately, LORETA software cannot perform a multivariate regression analysis, so the pure effect of duration of CI use and age of implant could not be determined).

Time course analysis showed that both frontal areas and cingulate cortex were generally less activated in patients than in controls, with no cyclic pattern attributable to ERPs elicitation (Mulert et al, 2004), which is clearly apparent in all control groups. This cyclic pattern of activation showed two maxima, corresponding to the N200 and P300 peaks. From a neurophysiological point of view, this result suggests that the control group had a temporally ordered activation of the cingulate and frontal areas, but such an organization was not apparent in the patient group, probably due both to a more limited activation and to a temporal disorganization.

Except in C patient group, the maximum corresponding to the P300 peak was more or less evident in patients and controls, while the maxima corresponding to the N200 peak were virtually absent in all patient groups. This is consistent with the grand average ERP analysis, in which the N200 peak was found to be less well-defined in patients than in controls.

This, despite the fact that the patients belonging to the prelingual A group and postlingual D group (and to a lesser extent the B patient group) showed an almost similar activation in strength and timing of these cortical areas, compared to controls.

As regards the EEG signal, functional connectivity showed a significant increase in the second and third prelingual patient group (B and C). This result was mainly observed in the alpha frequency range, during the activation state, and specifically between visual areas and Precuneus and posterior cingulate cortex.
An important characteristic of alpha rhythms is that they are seem to support top-down processing, providing high level of integration between different cortical regions (Von Stein and Sarnthein, 2000).
This increase in connectivity in the visual areas may suggest a sort of residual access to a sensory modality that compensates for the auditory modality before the implant.
In this respect, it is quite crucial that , even in this analysis, postlingual patients (group D) and patients with early implantation and long CI use (group A) showed no difference compared to controls.

# 6. Conclusion

Cochlear implant adds a new auditory modality in prelingual patients, allowing the creation of a functional network. This involves the areas implicated in sensory and cognitive modalities, and needs some time to form. In this sense, these results showed a great importance of a long use of the device in addiction to an early time of implant.
Indeed, our data suggest that even in case of late-implant (group B), the prolonged CI use may allow a normalization process to be developed, from both an audiological and a neurophysiological point of view.
Instead, in the case of patients with postlingual hearing loss, cochlear implant restores and reinforces a cortical network that has already been formed, before the onset of the hearing impairment.

The main limitations of the present study are the not very large sample size, the lack of a group of early-implanted patients with a short period of CI use, and the limited number of channels. The chance to study early-implanted patients with a short use of their CI collides with the feasibility of administering a P300 paradigm to very young children. The number of EEG channels does not allow for a high spatial resolution. However, these results showed a strong significance with regard to the specific question taken into account. Therefore, various examples of the use of 19 channels in the ERPs

cortical source analysis are available in the scientific literature. (Saletu and Anderer 2008; Van Duynslaeger et al, 2007, Calabrò et al, 2017).

In any case, this study provides interesting perspectives for future development, with the possibility to solve the current limitations and the opportunity to extend the scope, improving the knowledge in this field even more.

# References


- Emanuel, Diana & Maroonroge, Sumalai & Letowski, Tomasz. Auditory function: Physiology and function of the hearing system. 2009; 307-334.

- Alberti, Peter W. The anatomy and physiology of the ear and hearing. Occupational exposure to noise: Evaluation, prevention, and control. 2001; 53-62.

- Prosser S, Martini A. Argomenti di Audiologia. 2007; Omega Edizioni.

- Shearer AE, Hildebrand MS, Smith RJH. Hereditary Hearing Loss and Deafness Overview. 2017; In Adam MP, Ardinger HH, Pagon RA, et al., editors. GeneReviews.

- Gates GA, Miyamoto R.T. Cochlear Implants. The New England Journal of Medicine. 2003; 349, 421-423

- Ramsden R. and Graham J. Cochlear Implantation. BMJ. 1995; 311, 1588

- Dhanasingh A, Jolly C. An overview of cochlear implant electrode array designs. Hearing Research. 2017; Volume 356 Pages 93-103.

- Zeng F.G, Rebscher S. Cochlear Implants: System Design, Integration and Evaluation. 2009; IEEE Rev Biomed Eng 1: 115–14.

- Tang Q, Li Y. MRI compatibility and safety of cochlear implants. Journal of Central South University. Medical sciences 2012; 37(3):311-5

- Crane BT, Gottschalk B, Kraut M, Aygun N, Niparko JK. Magnetic resonance imaging at 1.5 T after cochlear implantation. Otol Neurotol 2010; 31(8): 1215-20.

- May-Mederake B. Early intervention and assessment of speech and language development in young children with cochlear implants. Int J Pediatr Otorhinolaryngol. 2012; 76(7): 939-46.

- Niparko JK, Tobey EA, Thal DJ, Eisenberg LS, Wang NY, Quittner AL. Fink NE. Spoken language development in children following cochlear implantation. JAMA. 2010; 21;303(15):1498-506.

- Sharma A, Dorman MF, Spahr AJ. A sensitive period for the development of the central auditory system in children with cochlear implants: implications for age of implantation. Ear Hear. 2002; 23(6): 532–39.

- Gordon KA, Wong DDE, Papsin BC. Bilateral input protects the cortex from unilaterally-driven reorganization in children who are deaf. Brain 2013; 136: 1609–25.

- Sharma A, Dorman MF, Kral A. The influence of a sensitive period on central auditory development in children with unilateral and bilateral cochlear implants. Hear Res 2005; 203(1-2): 134–43.

- Kral A, Yusuf PA, Land R. Higher-order auditory areas in congenital deafness: Top-down interactions and corticocortical decoupling. Hear Res. 2016; S0378-5955(16)30163-0.

- Kral A, Kronenberger WG, Pisoni DB, O'Donoghue GM. Neurocognitive factors in sensory restoration of early deafness: a connectome model. Lancet Neurol 2016; 15(6): 610–21.

- Kral A, Yusuf PA, Land R. Higher-order auditory areas in congenital deafness: Top-down interactions and corticocortical decoupling. Hear Res 2017; 343: 50-63.

- Stropahla M, Ling-Chia C, Debenerab S. Cortical reorganization in postlingually deaf cochlear implant users: Intra-modal and cross-modal considerations. Hear Res 2017; Volume 343, Pages 128-137

- Crosson B, Ford A, McGregor K, Meinzer M, Cheshkov S, Li X, Walker-Batson D, Briggs RW. Functional Imaging and Related Techniques: An Introduction for Rehabilitation Researchers. J Rehabil Res Dev. 2010; 47(2): vii–xxxiv

- He B, Yang L, Wilke C, Yuan H. Electrophysiological Imaging of Brain Activity and Connectivity – Challenges and Opportunities. IEEE transactions on bio-medical engineering. 2011; 58(7):1918-1931.

- Megías M, Emri Z, Freund TF, Gulyás AI. Total number and distribution of inhibitory and excitatory synapses on hippocampal CA1 pyramidal cells. Neuroscience. 2001; 102 (3): 527–40.

- Barnett MW, Larkman PM. The action potential. Pract Neurol. 2007; 7 (3): 192–7. PMID 17515599.

- Lopes da Silva F. EEG: Origin and measurement. EEG-fMRI: Physiological Basis, Technique, and Applications. 2010; 19-38. 10.1007/978-3-540-87919-0_2.

- Harpale VK, Bairagi VK. Time and frequency domain analysis of EEG signals for seizure detection: A review. 2016; International Conference on Microelectronics, Computing and Communication, MicroCom 2016, art. no. 7522581.

- Kropotov JD. Functional Neuromarkers for Psychiatry. Applications for Diagnosis and Treatment. 2016; Pages 399–402. Chapter 7.1 – Objective Measures of Human Brain Functioning.

- Sur S, Sinha VK. Event-related potential: An overview. 2009; Ind Psychiatry J. 18(1): 70–73

- Reis AC, Frizzo AC, Isaac Mde L, et al. P300 in individuals with sensorineural hearing loss. Braz J Otorhinolaryngol. 2015; 81: 126-132.

- Perez AP, Ziliotto K, Pereira LD. Test-Retest of Long Latency Auditory Evoked Potentials (P300) with Pure Tone and Speech Stimuli. Int Arch Otorhinolaryngol. 2017; 21(2): 134–139.

- Grech R, Cassar T, Muscat J, Camilleri KP, Fabri SG, Zervakis M, Xanthopoulos P, Sakkalis V, Vanrumste BJ. Review on solving the inverse problem in EEG source analysis. Neuroeng Rehabil. 2008; 5: 25.

- Pascual-Marqui RD, Esslen M, Kochi K, Lehmann D. Functional imaging with low resolution brain electromagnetic tomography (LORETA): a review. Methods Find Exp Clin Pharmacol 2002; 24 Suppl C:91-5.

- Pascual-Marqui R.D, Michel CM, Lehmann D. Low resolution electromagnetic tomography: a new method for localizing electrical activity in the brain. Int J Psychophysiol. 1994; 18(1):49-65.

- Talairach J, Tournoux P. Co-Planar Stereotaxic Atlas of the Human Brain. 1988; Stuttgart, Germany: Georg Thieme.

- Pascual-Marqui RD. Standardized low-resolution brain electromagnetic tomography (sLORETA): technical details. Methods Find Exp Clin Pharmacol. 2002; 24 Suppl D:5-12.

- Towle VL, Bolanos J, Suarez D, Tan K, Grzeszczuk R, Levin DN, Cakmur R, Frank SA, Spire JP. The spatial location of EEG electrodes: Locating the best-

fitting sphere relative to cortical anatomy. Electroencephalogr. Clin. Neurophysiol. 1993; 86: 1–6.

- Babiloni C, Del Percio C, Boccardi M. Occipital sources of resting state alpha rhythms are related to local gray matter density in subjects with amnesic mild cognitive impairment and Alzheimer's disease. Neurobiol Aging. 2015; 36(2): 556–570.

- Pascual-Marqui RD, Lehmann D, Koukkou M. Assessing interactions in the brain with exact low-resolution electromagnetic tomography. Phil. Trans. R. Soc. A 2011; 369, 3768–3784.

- Bowyer SM. Coherence a measure of the brain networks: past and present. Neuropsychiatric Electrophysiology 2016; 2:1.

- Peraza LR, Asghar AU, Green G, Halliday DM. Volume conduction effects in brain network inference from electroencephalographic recordings using phase lag index. J Neurosci Methods. 2012; Volume 207, Issue 2, 189-199.

- Vega CF, Noel J. Parameters analyzed of Higuchi's fractal dimension for EEG brain signals. 2015; published in: Signal Processing Symposium (SPSympo).

- Zeng FG, Trends in Cochlear Implants. Trends Amplif. 2004; 2004;8(1):1-34.

- Dobie RA, Van Hemel S. Hearing Loss: Determining Eligibility for Social Security Benefits. 2004; National Research Council (US) Committee on Disability Determination for Individuals with Hearing Impairments. Editors. Washington (DC): National Academies Press (US).

- Mondini s. Esame neuropsicologico breve. Una batteria di test per lo screening neuropsicologico. Cortina Raffaello, 2003.

- Uddin LQ, Kelly AM, Biswal BB, Castellanos FX, Milham MP. Functional connectivity of default mode network components: correlation, anticorrelation, and causality. Hum Brain Mapp. 2009; 30(2).

- Raichle ME, MacLeod AM, Snyder AZ, Powers WJ, Gusnard DA, Shulman GL. A default mode of brain function. Proc Natl Acad Sci U S A. 2001; 98(2):676-82.

- Blumenfeld H. Neuroanatomical Basis of Consciousness, in The Neurology of Conciousness (Second Edition), 2016; Cognitive Neuroscience and Neuropathology, Pages 3-29.

- Spreng RN. The Fallacy of a "Task-Negative" Network. Frontiers in Psychology. 2012; 3:145.

- Cavanna AE, Trimble MR. The precuneus: a review of its functional anatomy and behavioural correlates. Brain. 2006; Volume 129, Issue 3, Pages 564–583.

- Merabet LB, Pascual-Leone A. Neural Reorganization Following Sensory Loss: The Opportunity of Change. Nature reviews Neuroscience. 2010;11(1):44-52.

- Sharma A, Glick H. Cortical Neuroplasticity in Hearing Loss: Why It Matters in Clinical Decision-Making for Children and Adults. Audiology & Neuroscience. 2018; Hearing Review.

- Mulert C, Pogarell O, Juckel G, et al. The neural basis of the P300 potential. Focus on the time-course of the underlying cortical generators. Eur Arch Psychiatry Clin Neurosci 2004; 254(3): 190–98

- Von Stein A, Sarnthein J. Different frequencies for different scales of cortical integration: from local gamma to long range alpha/theta synchronization. Int J Psychophysiol. 2000; 1;38(3):301-13.

- Saletu M, Anderer P. Event-related-potential low-resolution brain electromagnetic tomography (ERP-LORETA) suggests decreased energetic resources for cognitive processing in narcolepsy. Clin Neurophysiol 2008; 119(8):1782-94;

- Van Duynslaeger M, Van Overwalle F, Verstraeten E. Electrophysiological time course and brain areas of spontaneous and intentional trait inferences. Soc Cogn Affect Neurosci 2007; 2(3):174-88;

- Calabrò RS, Naro A, Manuli A, et al. Pain perception in patients with chronic disorders of consciousness: What can limbic system tell us? Clin Neurophysiol 2017;128(3):454-62.